NASA CR-135432

CREEP OF OXIDE DISPERSION STRENGTHENED MATERIALS (WITH SPECIAL REFERENCE TO T. D. NICHROME)

Jerhong Lin and Oleg D. Sherby

Stanford University
Stanford, California 94305

Prepared for

National Aeronautics and Space Administration
Lewis Research Center
Cleveland, Ohio 44135
June 1978
Grant NGR-05-020-671

INTRODUCTION

Creep of crystalline solids has been the subject of many studies, and research in the past twenty years has lead to a clarification of the important mechanisms controlling creep at temperatures above about 0.4 T_m. The major factors influencing the steady state creep rate of polycrystalline metals and metallic alloys are the diffusion coefficient of atoms, the elastic modulus, the subgrain size and the stacking fault energy[1-4]. When the grain size is very fine (1 to 50μm) it too plays an important role[1,5].

Dispersion hardening is considered one of the most potent methods of strengthening metals for elevated temperature service[1-3]. The exact mechanism for such strengthening, however, is not well understood. Two creep characteristics have generally been noted for dispersion hardened materials that seem to make them dissimilar from metals and metallic alloys. These are that the stress exponent, n, for creep is high[1,6-9] (generally greater than the value observed for metals that are controlled by a diffusion controlled slip creep process where $n \simeq 5$), and the activation energy for creep, Q, is usually greater than that for lattice diffusion[1,8,9]. These two parameters, n, and Q, are determined from the relation,

$$\dot{\varepsilon} = K \sigma^n \exp - \frac{Q}{RT} \qquad (1)$$

where $\dot{\varepsilon}$ is the steady state creep rate, K is a material constant, R is the gas constant, T is the absolute temperature and σ is the creep stress.

In recent years the high activation energy observed for many dispersion hardening systems was resolved when the modulus variation with temperature was taken into account[10-12]. This factor was shown to be important in pure metals earlier[13]. The modulus correction factor is directly proportional to the stress exponent, n, and is thus large for dispersion hardened alloys.

This correction yielded Q values which were equal to the activation energy for matrix self diffusion. This simplification permits rewriting equation (1) as

$$\dot{\varepsilon} = K D_L (\sigma/E)^n \qquad (2)$$

where D_L ($= D_{oL} \exp - \frac{Q_L}{RT}$) is the lattice self diffusion coefficient and E is the dynamic unrelaxed average Young's modulus. The stress exponent, n, was commonly noted to be about 7 to 10[1,14,15] and at times considerably higher[16].

Several authors have attempted to rationalize high values of the stress exponent by introducing various factors. Barrett was among the first[17] to point out that the measured stress exponent can be made to decrease by replotting data as $\log \dot{\varepsilon}/D_L$ versus $\log (\sigma-\sigma_o)$ where σ_o is a friction or threshold stress. Wilshire and his colleagues[18-20] attempted to explain steady state creep data for many crystalline solids with stress exponents greater than four by determining the appropriate σ_o to obtain the following generalized relation at a given temperature,

$$\dot{\varepsilon}_s \propto (\sigma-\sigma_o)^4. \qquad (3)$$

Wilshire and his colleagues then postulated that σ_o was a "friction stress" which represents the stress supported by substructural factors other than the dislocations taking part in the creep deformation process. The stress exponent of four is intended to indicate that a specific creep mechanism is operative, presumably one involving a diffusion controlled dislocation process. This concept, indeed, does have an attractive feature wherein a universal stress exponent apparently results. A negative feature to the approach is that, thus far, the value of σ_o cannot be calculated, apriori, either from observed microstructural features or from theoretical deductions for any given metal system. Thus, σ_o remains an empirical constant derivable only from doing

creep experiments. That is, the equation lacks predictive ability*. Another objection to the proposed relation, equation (3), is that it is not applicable to the many metals that exhibit a power law relation $\dot{\varepsilon}_s \alpha \sigma^n$ where n is a constant greater than 4 over many orders of magnitude of creep rate [4,22].

In an extension of the Wilshire et al. approach to complex materials, Evans and Harrison[23] indicated the added complication that σ_o needs to be stress dependent if a power law relation is to be preserved. For optimal correlation of their data, the authors showed that n should be 3.5 rather than 4. They also showed that σ_o was linearly dependent on stress at low stresses but essentially constant at high stresses. Following the method of Wilshire et al.[18-20], the value of σ_o was determined experimentally by decreasing the stress, after steady state creep was achieved at a given stress, to a stress where creep was considered to cease. The major uncertainty in the approach used by Evans and Harrison is the same as that mentioned earlier for the work of Wilshire et al. The value of σ_o, thus far, cannot be predicted without resorting to creep experiments. That is, it is not predictive.

Lagneborg and Bergman[24] analyzed the creep behavior of precipitation-hardened alloys which exhibited n values close to 4 at low stresses and to about 10 at high stresses. They developed a dislocation model which lead to a relationship of the type given by equation (3) where σ_o represented a back stress due to the particle dispersion. The authors showed that σ_o was a constant at high stresses but decreased linearly with stress at low stresses. Although their model may be correct for the materials they studied, it cannot account for the typical behavior of dispersion hardening materials where the

* The same objections are applicable to the approach used by Shewfeld and Brown[21] in their studies on Cu-SiO_2 and Cu-Al_2O_3 dispersion hardened materials. They propose a relation of the form $\dot{\varepsilon} \alpha \exp A(\sigma-\sigma_o)$ where A and σ_o are material constants which do not seem to be readily predictive.

stress exponent, n, is often either constant over a wide range of stress [1,14,15] or increases in magnitude with diminishing stress[16].

A different, and rather ingenious, concept was recently developed by Lund and Nix[16] to explain the creep behavior of oxide dispersion hardened materials. They studied single crystalline dispersion strengthened Nichrome. Their work led them to conclude that the high strength of such oxide dispersion strengthened alloys is due to the additive contribution of two terms: the stress to induce plastic flow in the matrix of the O.D.S. alloy (i.e., matrix devoid of particles) and the stress for dislocation bowing around the particles, i.e. the Orowan bowing stress. The latter stress is considered athermal and is called the threshold stress. For a given value of the diffusion compensated strain rate, $\dot{\varepsilon}/D_L$, their prediction is given mathematically as,

$$\left.\frac{\sigma}{E}\right|_{\text{T-D Nichrome}} = \left.\frac{\sigma}{E}\right|_{\text{Nichrome}} + \left.\frac{\sigma}{E}\right|_{\text{Threshold}}. \qquad (4)$$

Lund and Nix show excellent prediction of their T-D Nichrome data by this approach. The signifcance of their idea is clear. It is predictive. Only two characteristics need be known, one is the steady state creep behavior of the matrix material. The other is a knowledge of the microstructure of the dispersion hardened material (i.e. the mean free path between particles).

Another method of writing the Lund-Nix relation is as follows:

$$\dot{\varepsilon}_s = A\, D_L \left(\frac{\sigma-\sigma_o}{E}\right)^n , \qquad (5)$$

where n is the stress exponent for the matrix material (for Nichrome it is about 5) and A is the pre-exponential constant for the matrix material.

Although the Lund-Nix approach for explaining the creep behavior of O.D.S. alloys is very plausible, there are two possible objections. The first is that

their approach would dictate that the general creep behavior of dispersion hardened material is the same as that of the matrix per se. This may not be so, inasmuch as the matrix material (e.g. Nichrome) exhibits primary creep which is a function of the stress (decreasing in magnitude of strain with decreasing stress) whereas the O.D.S. material (e.g. T-D Nichrome) exhibits virtually no strain hardening over a wide range of stress. A second objection is that the threshold stress seems to be more difficult to determine microstructurally than originally thought[25,26].

The above general remarks indicate the various approaches used to analyze the behavior of O.D.S alloys. It is clear that although some rather important strides have been made recently, many questions remain unanswered. The purpose of this paper is to evaluate the creep behavior of T-D Nichrome, of different grain sizes and grain aspect ratios (G.A.R.), over the temperature range 900 to 1200°C. Tests were performed in compression in order to avoid complications arising from void and crack formation at grain boundaries during creep flow. Grain boundary separation, with low elongation to fracture, is a common occurrence in such materials when tested in tension at elevated temperature[15]. In fact, Whittenberger has shown that small tensile strains during elevated temperature creep will lead to brittle intergranular failure during subsequent testing at room temperature[27]. It was thought that stress-strain curves obtained in compression could lead to stress-strain rate relations representative of plastic flow processes which would exclude complications arising from void and crack formation and grain boundary deformation. The resulting data are then compared with other published results on T-D Nichrome and analyzed in the light of contemporary ideas on the possible importance of atom mobility, subgrain and dislocation structure, threshold stress and grain aspect ratio on the creep properties of O.D.S alloys.

MATERIALS AND EXPERIMENTAL PROCEDURE

T-D Nichrome was received from Dr. J. Daniel Whittenberger in the form of 6.35 mm (0.25 in) thick rolled plate as well as in 12.7 mm (0.5 in) extruded bar. The nominal composition of the material was 2% ThO_2, 20% chromium and the balance nickel. These materials were made and processed by Fansteel Corporation. The thermal-mechanical processing history was proprietary and led to dissimilar microstructures. The plate exhibited a banded structure of particle-rich and particle-poor regions. The extruded bar exhibited a uniform distribution of thoria particles in the Nichrome matrix.

Compression samples, 9.53 mm (0.375 in) in length and 6.35 mm (0.25 in) in diameter were prepared from the plate with the long axis in the longitudinal direction (of rolling) as well as in both the short and long transverse directions. Samples in the short transverse direction were made proportionately smaller. These samples were tested in the as-received condition and are designated as fine grain size samples in this paper. The grains were about 30μm by 70μm in dimensions giving a grain aspect ratio (G.A.R.) of about two. The as-extruded bar was heated to obtain a coarse grain size by heating from 1204°C (1200°F) to 1343°C (2450°F). The grains were about 100μm by 300μm in dimensions giving a G.A.R. of three. Compression samples were prepared of the same dimensions as for samples prepared from the plate. Samples were machined both in the longitudinal and transverse directions.

Tests were performed in compression in an Instron machine. Alumina push rods were used for compression testing. Boron nitride was used for lubrication and a Nichrome wound resistance heating furnace was used to heat samples in the range 900°C to 1200°C. All tests were performed in air. In a typical test the sample was heated to a fixed temperature and maintained at temperature for one hour. The sample was then deformed at a fixed crosshead speed until a strain

of about 3% was achieved at which point the strain rate was then changed to a new strain rate. This procedure was repeated to a third strain rate. Testing was stopped at a total strain of 10 to 15%. A majority of the samples tested deformed quite uniformly (i.e. no macroscopic anisotropic flow occurred). The deformed samples were examined for evidence of cracking or sheared features. For transmission electron microscopy studies the as-received and deformed samples were cut in slices normal to the direction of compression by a low speed diamond saw (Isomet). Discs with a diameter of 3mm were punched out from the center of these slices. These slices were then electropolished in a solution of 20% perchloric acid in ethanol in the temperature range of $-15^{o}C$ to $-8^{o}C$. A Phillips 200 electron microscope was used, and a dark field technique was employed to study the subgrain structure.

RESULTS AND DISCUSSION

A typical example of the true stress - true strain behavior of T-D Nichrome at elevated temperature is shown in Figure 1. The example shown is for coarse grained T-D Nichrome at $1000^{o}C$ where the material is plastically deformed at various cross-head speeds. It will be noted that a small amount of strain hardening occurs initially, to about one percent, followed by little or no strain hardening, i.e. a steady state flow stress seems to be achieved. Subsequent tests on the same sample at both lower and higher strain rates than the initial rate revealed new flow stresses that were essentially invariant with strain. That is, the structure important to creep did not significantly change with straining irrespective of the stress level. Such results were typical of those obtained for the coarse grain size materials at all temperatures of testing, i.e. 900 to $1200^{o}C$. Tests were stopped when total true strains of about 0.12 to 0.15 were reached. This was done because non-uniform compression flow,

in the form of barrelling, became visibly evident at strains exceeding $\varepsilon \simeq .15$ and the calculated stress under these conditions were not considered reliable. Longitudinal surface cracks were occasionally observed at strains in the order of $\varepsilon \simeq 0.15$ only at 1200°C.

Fine grain size T-D Nichrome behaved in a manner quite similar to the coarse grain size material in that no significant hardening or softening occurred during straining in the strain rate-change tests performed. Exceptions were fine grain specimens tested at 1200°C, and occasionally at 1100°C, where strain softening was observed. No significant changes in microstructure occurred after strain softening when samples were examined by electron microscopy studies. Thus, the origin of strain softening was not obvious but might be related to the banded microstructure noted in the fine grain T.D. Nichrome.

The flow stress-strain rate data obtained from tests of the type shown in Figure 1 are recorded in Table I for fine grain size T-D Nichrome and in Table II for coarse grain size T-D Nichrome. The data at 1200°C for the fine grain size T-D Nichrome are the maximum flow stresses observed since strain softening occurred.

Analysis of T-D Nichrome and Comparison with other Published Data

The flow stress-strain rate data for fine grain size T-D Nichrome is plotted on a log-log scale in Figure 2. Data for all three test directions are included for all temperatures investigated. Three major findings can be noted.

The first is that no anisotropy in properties or in specimen shape were noted in the T-D Nichrome. That is, in spite of the grain shape anisotropy, this characteristic did not influence the creep properties or the specimen shape in the different directions of testing. This result would suggest that it is the structure within the grains that is controlling the creep strength of T-D Nichrome during compression deformation.

The second characteristic noted for the fine grain T-D Nichrome is that a power law relation is obeyed over almost the whole stress range studied, where the stress exponent, n, is about eight. This particular value is the same as that observed in metals where the stress exponent was determined under constant structure[4]. This point will be discussed in detail in a subsequent section.

The third observation is that the activation energy for creep [using equation (1)] is about 400 kjoules per mole, a value considerably above that for nickel lattice diffusion in Nichrome, Q = 285 kjoules per mole[28]. This high activation energy for creep is accounted for by the temperature variation of the elastic modulus[10-13]. The influence of temperature on the modulus of nichrome containing thoria particles has been studied both in the polycrystalline form as well as in single crystalline form by several investigators[29,30]. These data are reported in Figure 3. The polycrystalline modulus data was used by us to assess the temperature dependence of creep. Thus, Figure 4 shows a plot of the fine grain size T-D Nichrome data as logarithm of the creep rate versus logarithm of the modulus compensated stress, σ/E. The activation energies for creep are given in parentheses at different stresses and temperatures. As can be seen, the average activation energy is 270 kjoules per mole, a value essentially equal to that for nickel lattice diffusion in Nichrome.

The coarse grain size T-D Nichrome behaved quite differently from the fine grain size material. A plot of logarithm $\dot{\varepsilon}$ versus logarithm σ/E is shown for the coarse grain size material in Figure 5. As can be seen, whereas the stress exponent is about eight at high stresses, it increses with decreasing stress and is in the order of 25 at the lowest stresses studied. Such a trend is indicative of a threshold stress. The activation energy for creep of the coarse grain size material was found to be 285 kjoules per mole. This value is nearly the same as that observed for the fine grain size material (Figure 4). The limited tests performed on the influence of anisotropy on the creep rate of coarse grain T-D

Nichrome reveal virtually no difference in strength with direction of testing; in this case the G.A.R. was about three. Again these results would suggest that compression creep flow in coarse grain T-D Nichrome is controlled by mechanisms occurring within the grains of the material.

The two T-D Nichrome samples studied are compared in Figure 6 by plotting the diffusion compensated creep rate versus the modulus compensated stress. It can be seen here that coarse grained T-D Nichrome is considerably stronger than fine grained T-D Nichrome. The difference in strength is difficult to rationalize based on microstructural differences, but can be quantitatively correlated if a difference in threshold stress exists for the two materials. Whittenberger[33] has presented an empirical correlation between the threshold stress and the G.A.R. for several O.D.S. alloys wherein the threshold stress increases as the G.A.R. increases. More discussion on this point will be presented later.

The processing of the coarse grain size material into bar lead to a highly textured state: a [100] texture parallel to the bar axis with the [010] and [001] directions more or less randomly oriented about the [100] was obtained[34]. The fine grain size material, processed as plate, was much less severely textured. Since the modulus of T-D Nichrome is a strong function of orientation (see Figure 3). it might be tempting to consider this factor as a possible variable in analyzing the creep data. Studies on fcc and bcc metals, however, have shown rather convincingly that texture does not appear particularly important in power-law creep. For instance, Barrett, Lytton and Sherby[35] found only a factor of two difference in creep rate between textured and randomly-oriented copper; similar results were noted for the creep rate of textured iron-silicon[32,36]. In both instances the modulus anisotropy is quite large and similar to that observed for T-D Nichrome (Figure 3). This isotropic behavior in creep is, of course, expected since the creep rate would be dictated by the shear stress on the sample if slip is the principal mode of deformation. And, both bcc and fcc metals exhibit many slip systems

allowing slip to occur at or near the maximum shear stress direction. [Some authors use the shear modulus in the active slip plane and direction as the correct modulus to use in plots of the type given in Figures 4, 5 and 6. We believe, however, that the average modulus should be used based on the following argument. Dislocation climb is believed to be the rate controlling process in steady state creep when slip is the principal mode of plastic flow[2]. The rate of climb would be dictated by the elastic stress fields of obstacles in the path of the moving dislocation (e.g. subgrain boundaries, other dislocation arrays, and even perhaps particles). The nature of the obstacle would be of a random form and therefore the average obstacle would likely be associated with the average modulus in the crystal.] We thus find strong justification for our use of the average unrelaxed polycrystalline modulus in the dimensionless parameter σ/E in correlations of steady state creep behavior of polycrystalline materials (Figures 4, 5 and 6).

Figure 7 compares the results of our fine and coarse grain size materials with those obtained by other investigators on the tensile creep of T-D Nichrome. The averaged creep behavior of Nichrome as obtained by three separate investigators [37-39] is also included in Figure 7. The behavior of Nichrome is typical of that expected in Class II solid solution alloys[3]. That is, the stress dependence is about five. Such solid solutions generally exhibit large primary creep strains; in addition, the development of equilibrium subgrain structures that are uniquely dependent on the stress are generally observed. Certain interesting trends can be noted in Figure 7. Our coarse grain size material tested in compression virtually superimpose on the single crystal data of Lund and Nix, as well as on the single crystal data of Kane and Ebert[40]. This suggests that these materials may exhibit approximately the same microstructural features even

though the single crystalline materials were prepared by General Electric Company by directional recrystallization. Both the coarse grain and single crystalline materials exhibit high stress exponents at low stresses suggestive of the presence of a threshold stress. The remaining data, namely our fine grain size T-D Nichrome, the tensile creep data of Kane and Ebert[40], and the two sets of tensile data of Wilcox and Clauer[41], exhibit stress exponents in the order of seven to ten. The difference in strength among the various T-D Nichrome samples must be attributed to differences in microstructure and also possibly to the mode of testing (i.e. compression or tension).

Many O.D.S.alloys exhibit stress exponents in the order of eight. In Figure 8 we plotted data for Cu-Al_2O_3, αU-Al_2O_3, Mg-MgO, Al-Al_2O_3 and Ni-Al_2O_3 [42-46]. We also include our fine grain T-D Nichrome data for comparison. The data are plotted as $\dot{\varepsilon}/D_{eff}$ versus σ/E where D_{eff} is the effective diffusion coefficient which incorporates the contribution of lattice diffusion and dislocation pipe diffusion to the overall diffusion process[22,55-58]. The resulting correlation is gratifying from the viewpoint that the data at various temperatures superimpose on a common line for a given material and the slope of the resulting lines is about nine*. The data for Mg-MgO is especially impressive for it covers over eight orders of magnitude of the diffusion compensated strain rate. The original data from each investigation is given in the appendix; the method of determining D_{eff} (only for the Mg-MgO data was diffusion along dislocations important) is also described in the appendix.

* Other data on O.D.S. alloys were found which were not reported. For example, stress-rupture data have been reported for Ni-Al_2O_3 alloys by Schafter, Quatinez and Weeton[59]. And, stress rupture data have been reported for a new Cu-Al_2O_3 composite developed by Glidden-Durkee commercially known as Glidcop[60]. In both cases, the log stress versus log rupture time relation yielded a slope equal to about negative 9. These results are in quantitative agreement with those reported in Figure 8 since it is well accepted that $\dot{\varepsilon}_s$ and t_r are reciprocally related (i.e. the Grant-Monkman relation[61] reveals that $\dot{\varepsilon}_s = C/t_r$ where C is a constant for a given material).

Analysis of the O.D.S. Alloys on the Basis of Constant Structure and Threshold Stress.

It is our contention that many dilute dispersion hardened materials have within them a fine dislocation substructure, generally created by the prior thermal-mechanical history used in processing the material. Furthermore we propose that this dislocation structure is stabilized by the presence of the particles and is invariant with the creep stress applied at elevated temperature. This suggestion is in agreement with the absence of transient hardening or softening upon a change in stress (Figure 1). This reasoning would suggest that the stress exponent for such materials should be compared with the stress exponent obtained in constant structure tests for pure metals. Such tests can be performed by either strain rate change tests in constant strain rate tests[62] or stress-change tests (dip tests) in creep tests[63-67]. An example of such tests from a number of investigations for high purity aluminum is shown in Figure 9. The subgrain size which characterizes the constant structure for the tests performed is given for each investigation. As can be seen the slope is about eight rather than about five, the value noted when steady state creep rates are plotted as a function of stress[1-3]. These tests permit a deduction of the influence of subgrain size per se on the creep rate (we assume that the dislocation density within the subgrains does not significantly influence the creep strength). Such tests lead to the development of the following phenomenological relation for the creep rate[4],

$$\dot{\varepsilon} = K \left(\frac{\lambda}{b}\right)^3 \frac{D'_L}{b^2} \left(\frac{\sigma}{E}\right)^8, \qquad (6)$$

where λ is the subgrain size and b, the burgers vector, is introduced to permit the material constant K to be unitless. It was suggested that $K = 10^9$ for

high stacking fault energy materials. Equation (6) predicts that all the constant structure tests for aluminum shown in Figure 9 should superimpose when plotted as $\frac{\dot{\epsilon}}{D\lambda^3}$ versus σ/E with a slope equal to eight. This is verified by such a plot in Figure 10.

It is proposed that equation (6) is applicable to explaining the strength of O.D.S. alloys. First, a predicted stress exponent of eight is comparable to the stress exponents observed for many O.D.S. alloys (Figure 8). Second, lattice diffusion and the elastic modulus is predicted to be important which has already been verified to be the case (Figures 4,6 and 8). And, third, a structural feature, λ, is included as a potential variable to explain the high strength of the O.D.S. alloys. In pure metals, λ is the subgrain size which represents the barrier distance for dislocation motion. In the case of dispersion hardened materials, λ can be associated with the subgrain size or with the particle spacing, since the latter may be an effective barrier to dislocation motion. The difference in strength of the different T-D Nichrome materials studied (Figure 7) would thus be associated with the microstructural variable λ.

We show the application of equation (6) to the O.D.S. alloys (plotted in Figure 8) by showing the predicted logarithm $\dot{\epsilon}/D_{eff}$ versus logarithm σ/E curve forthree specific subgrain sizes in Figure 11. The correlation is gratifying in that the experimental curves fall within the subgrain size range of λ = 1μm to 0.1μm. Such values of subgrain size are commonly observed in O.D.S. alloys after normal thermal-mechanical processing [41,46,69,70]. The microstructures were not evaluated in the O.D.S. alloys shown in Figure 8 so that quantitative correlations were not possible; the fine grain T.D. Nichrome alloy studied in this investigation will be discussed in the next paragraph. Nevertheless the good correlation shown between equation (6) and

experimental data for O.D.S. alloys would suggest that this equation is quantitatively correct.

In the following we attempt to predict the mechanical behavior of our fine and coarse grain T-D Nichrome on the basis of equation (6). We will first analyze the fine grain size T-D Nichrome where a small threshold stress may exist which we will assume to be zero for our analyses. We will then analyze the coarse grain size T-D Nichrome where a threshold stress is introduced to assess the behavior of this material.

Figure 12 compares the creep behavior of Nichrome and our fine grained T-D Nichrome. The two curves intersect at $\sigma/E = 1.5 \times 10^{-3}$. This value of σ/E on the nichrome line permits us to predict the subgrain size in nichrome at this modulus compensated stress. This can be readily estimated from subgrain size-stress relations published for nickel[1,71,72], which we will assume to behave like nichrome. The nickel data are plotted in Figure 13 and yield $\lambda \simeq 3b\ (\sigma/E)^{-1}$. Since $b = 2.5\text{Å}$, λ is calculated to be 0.5μm. This is the predicted subgrain size in our fine grain T-D Nichrome if equation (6) is applicable and if subgrain size is the important microstructural feature for creep resistance in the O.D.S. alloys. Transmission electron microscopy studies in our fine grain size T-D Nichrome revealed a duplex structure. Subgrains 0.6μm in size were found mostly in groups. In total volume only about 20% of the material consisted of subgrains. If the flow stress for creep is controlled by the subgrain network then it might be concluded that our observed microstructure (λ = 0.6μm) agrees with our predicted microstructure (0.5μm). The reason why the small fraction of subgrains observed in the as-received material dominates the level of flow stress will be described later.

More positive evidence of the possible importance of subgrains on the creep of T-D Nichrome was found in our analyses of the coarse grain T-D

Nichrome. In this case, however, we had to consider the additional influence of a threshold stress. We chose a threshold stress to get the best possible straight line on a log-log plot, using a least squares analysis. The threshold stress value was $\sigma_o/E = 5.5 \times 10^{-4}$ and the resulting correlation is shown in Figure 14. In this figure we compare the creep rate-stress relation for coarse grain T-D Nichrome with nichrome. The first major observation is that the resulting straight line yields a slope nearly equal to eight, a stress exponent we associate with constant structure. The second major result is the predicted calculation of the subgrain size. In this instance the point of intersection was at $\sigma/E = 7 \times 10^{-4}$. At this value of stress over modulus, the equilibrium subgrain size is $\lambda = 1\mu m$ (Figure 13). Metallographic studies (Figure 15) of the as-received coarse grain material revealed a similar substructure to that observed in our fine grain T-D Nichrome. The subgrain size in this case, however, was equal to $1.2\mu m \pm 0.2\mu m$ [73]. About thirty percent of the material consisted of subgrains and tended to exist in clusters. The subgrain size observed is nearly equal to the predicted subgrain size by use of equation (6) and a threshold stress. This correlation attests to the possible validity of equation (6) modified by a threshold stress to yield the following generalized equation for creep of O.D.S. alloys

$$\dot{\varepsilon} = k \left(\frac{\lambda}{b}\right)^3 \frac{D_L}{b^2} \left(\frac{\sigma-\sigma_o}{E}\right)^8 \qquad (7)$$

where $\frac{\sigma_o}{E}$ is the modulus compensated threshold stress and K is a material constant equal to the constant K in equation (6) for the behavior of the matrix material exclusive of particles (at constant structure). We thus see that our approach is similar to Lund and Nix, except for one major factor. We consider that the strength of O.D.S. alloys can be determined by the additive contribution of the matrix strength at a given subgrain structure state

(rather than steady state structure as assumed by Lund and Nix) and the threshold strength.

Our interpretation of the results shown in Figure 14 yields an interesting new prediction. If constant strain rate tests are performed on the coarse grain T-D Nichrome above the intersection stress, then the stress-strain curve should exhibit strain hardening because the equilibrium subgrain size will be finer than the subgrain size for the as-received material ($\lambda \simeq 1\mu m$). That is, tests performed at strain rates and temperatures where $\dot{\varepsilon}/D$ is greater than $3 \times 10^{9} cm^{-2}$ (the modulus compensated strain rate at the intersection stress) (Figure 14), should exhibit strain hardening whereas tests performed below $\dot{\varepsilon}/D = 3 \times 10^{9} cm^{-2}$ should show negligible strain hardening. This prediction is borne out by a test performed by Hausselt and Nix[73] on the same coarse grain T-D Nichrome at $\dot{\varepsilon}/D = 4 \times 10^{12} cm^{-2}$. The stress-strain curve (plotted as σ/E versus ε) is shown in Figure 16 and compared to tests performed at $\dot{\varepsilon}/D$ values below the intersection stress. The contrast in stress-strain behavior is dramatic The test performed at $\dot{\varepsilon}/D = 4 \times 10^{12} cm^{-2}$ exhibits significant strain hardening whereas strain hardening is seen to be negligible in other tests. Our strain-rate change tests, shown in the same figure, reveal the same trend. It is possible to predict the increase in flow stress during straining in the strain hardening region (i.e. at $\dot{\varepsilon}/D = 4 \times 10^{12} cm^{-2}$) by means of our phenomenological relation, equation (7). Thus, this equation predicts that $(\frac{\sigma-\sigma_o}{E})$ is proportional to $\lambda^{-3/8}$ at constant strain rate and temperature. Hausselt and Nix showed that the subgrain size decreased from 1.2μm to 0.2μm at $\dot{\varepsilon}/D = 4 \times 10^{12} cm^{-2}$. This decrease leads to a predicted fractional increase of $(\frac{\sigma-\sigma_o}{E})$ equal to 1.96. The actual increase in the threshold-modified flow stress is 2.11. This good correlation gives further evidence for the validity of equation (7).

The above discussion permits us to predict the creep behavior of O.D.S. alloys at elevated temperature over a wide range of stress. Equation (7) predicts data in the stress range where the stress exponent is equal to eight. In this range the subgrain size is constant and equal to the as-received subgrain size. At high stresses, however, that is above the intersection stress, the equilibrium subgrain size is finer than the as-received subgrain size and the subgrain size will vary with stress. In this range, the appropriate variation of subgrain size with stress must be introduced into equation (7), and the stress exponent will decrease. Thus for T-D Nichrome, the following equation should be used in conjunction with equation (7),

$$\lambda \simeq 3b\left(\frac{\sigma-\sigma_o}{E}\right)^{-1} \quad . \tag{8}$$

We illustrate graphically the predicted variation of subgrain size with stress that we would use for describing the creep behavior of our coarse T-D Nichrome over a wide range of stress; this is shown in Figure 13 as solid lines. The data of Hausselt and Nix on the subgrain size observed in coarse grain T-D Nichrome is plotted against $\frac{\sigma-\sigma_o}{E}$ in the same figure. Their data agree with our predicted relation: that is, the data obtained at the highest stress falls on the line given by equation (8), and the two lowest stress data points lie near to the constant subgrain size line of 1μm given in the figure. These results help confirm our contention that the subgrain structure is about constant in the strain rate change tests we performed where the maximum creep strain was $\varepsilon \simeq 0.12$, and where $\dot{\varepsilon}/D$ was less than $3 \times 10^{9} cm^{-2}$.

We have emphasized subgrains as the principal barrier to plastic flow in O. D. S. alloys. The creep behavior of the T-D Nichrome above and below $\dot{\varepsilon}/D \simeq 3 \times 10^{9} cm^{-2}$ would appear to be strong evidence for this type of a postulate. And, we have

attributed the eight power law region as indication of the presence of a constant structure. This viewpoint, however, must be reconciled with the structural observation that only 20 to 30% of the initial structure consists of subgrains as in the case of the fine and coarse grain T-D Nichrome. It is our contention that the subgrain structure observed in the as-received material is a reflection of the barrier spacing controlling plastic flow of O.D.S. materials. In the regions where subgrains exist, it is the subgrain size that dictates the creep resistance; we noted in coarse grain T-D Nichrome that the subgrains generally were pinned by particles, or clusters of particles, in the size range 700 to 1000Å. In regions not containing subgrains, it is the spacing between specific size particles (700-1000 Å in coarse grain T-D Nichrome), equal to the spacing of the subgrain size, that controls the creep resistance. During extensive creep flow, dislocations would be expected to form subgrains in the originally subgrain-free region; the final size, however, would be no larger than the maximum subgrain size observed in the as-received material. In T.E.M. studies on coarse grain T-D Nichrome after creep deformation, we noted that subgrains would gradually develop in the subgrain-free regions which help to confirm the above remarks. For example, at a stress of $\frac{\sigma-\sigma_o}{E} = 3 \times 10^{-4}$, about 80% of the material consists of subgrains after 0.3 strain.

Another approach to understanding the creep behavior of O.D.S. alloys is to relate the strength to the dislocation density not associated with subgrains. Transmission electron microscopy studies by Hausselt and Nix reveal the influence of strain and stress on the dislocation density. They showed that the dislocation density builds up rapidly in the initial one percent strain and then remains constant thereafter. These dislocations are likely the "geometrically necessary" dislocations initially described by Ashby for dispersion hardened materials[74]. These dislocations should inhibit general dislocation motion and can lead to the small increase in flow stress

observed in the initial portion of the stress-strain curve (Figure 1) when tested at $\dot{\varepsilon}/D \leq 3 \times 10^{9}$ cm^{-2}. The dislocation density was shown to remain constant after the first percent of strain, but to be a strong function of stress, increasing with increase in stress. The steady state flow stress of T.D.-Nichrome is not readily explained through the variation of dislocation density with stress. Thus, transients in the form of strain hardening or strain softening should be observed in change-in-strain-rate tests if the dislocation density is an important variable. No such transients were observed (Figure 1). The subgrain strengthening concepts presented earlier seem to us to be a more readily useful one in describing the creep behavior of O.D.S. alloys.

We noted earlier that the coarse grain T-D Nichrome creep data superimposed on the single crystalline T.D. Nichrome data (Figure 7). Comparison of the particle distribution in the two materials indicates they are quite similar[16,73]. It was decided to test our phenomenological relation (equation 7) with respect to predicting the creep behavior of the T.D. Nichrome data since this material was studied over a very wide temperature and strain rate range. The same parameters as used for the coarse grain T-D Nichrome data were used, namely λ was chosen to vary as given in Figure 13 and $\frac{\sigma_o}{E}$ was chosen as 5.5×10^{-4}. The resulting prediction is given by the solid lines shown in Figure 17 and the experimental data are given by symbols. The prediction looks remarkably good and suggests that the concept of a structural spacing (in this case the subgrain size, λ), which is constant at low stresses but varies with stress at high stresses, is probably applicable for describing the creep behavior of single crystalline T.D. nichrome.

The determination of the threshold stress remains a mystery. Our analysis of several O.D.S. alloys in Figure 8 reveal, at least for these materials, that

the threshold stress, if it exists, must be quite small. Wilcox and Clauer[41,68] related the increase in high temperature strength in O.D.S. alloys by extensive mechanical working (by drawing) to the change in grain aspect ratio. They showed that the yield strength at 1100°C increased with increase in $\frac{L}{\ell}$ where L is the length of the grain in the direction of testing and ℓ is the transverse length of the grain. They attributed this effect to the importance of grain boundary sliding to the deformation process. They reasoned that elongated grains "would have a lower average shear stress resolved onto the grain boundaries than the equiaxed grains" and would therefore be more creep resistant[41]. There is some evidence that this concept may not be correct. For one, TEM studies[73] on coarse grain T-D Nichrome have revealed that the dislocation density increased significantly in the first percent of straining. This suggests that the primary mode of deformation in O.D.S. alloys is due to the dislocation motion within the grains. Thus, in tension creep tests with a total plastic strain of two percent normally obtained, we should not expect grain boundary sliding to be the principal deformation mechanism. For another, if grain boundary sliding is important in creep of O.D.S. alloys then strong anisotropy in creep properties could be expected; this was not observed in our studies of compressive creep in fine and coarse grain T-D Nichrome (Figures 4 and 5). The remarkably similar behavior of our coarse grain T-D Nichrome with the single crystalline T.D. nichrome would also suggest that grain boundary morphology does not play an important role in compressive creep of O.D.S. alloys. It is our contention that the grain aspect ratio (G.A.R.) is a measure of the change in microstructure that occurs in the sample through the thermal-mechanical processing treatment given to obtain various G.A.R. values. Increase in G.A.R. is usually accompanied by subgrain size refinement and by a change in particle morphology[75] (and also perhaps in size). Subgrain refinement would lead to strengthening of a type we predict

with equation (7). The change in particle morphology and size could lead to a change in the value of the threshold stress. Whittenberger has shown good experimental correlation between the threshold stress and the G.A.R. for various large grain size nickel-base O.D.S. alloys. We show his results in Figure 18, and add to it the threshold stress for our coarse grain size T-D Nichrome. A threshold stress can be calculated for our fine grain size material (by improving the slope from 9 to 8) and its value is also plotted in Figure 18. The high threshold stress for single crystalline T-D Nichrome cannot be plotted in the graph since the G.A.R., in this case, has no meaning.

Threshold stresses have been noted in dispersion hardened systems under conditions dissimilar from those mentioned above. Burton[76] worked with Cu-Al_2O_3 composites of varying alumina content (0.5, 1.0 and 1.5% Al_2O_3) at temperatures approaching $0.9T_m$ of pure copper. He calculated threshold stresses which were an order of magnitude below those discussed for T-D Nichrome (i.e. $\sigma/E = 0.65$ to 2.32×10^{-5}) and used these values to show that Nabarro-Herring creep may be controlling the deformation behavior of these composites. He associated the threshold stress with "particles that inhibit the action of boundaries as vacancy sinks and sources". Edwards, McNelley and Sherby[77] showed that threshold stresses are observed in large volume fraction particulate composites (e.g. Zn-30% Al_2O_3). Large threshold stresses were noted, $\sigma/E \simeq 10^{-3}$, and were related to the stress necessary to generate dislocations at particle-matrix interfaces. These large volume fraction composites exhibit properties that are quite dissimilar from the dilute dispersion hardened O.D.S. alloys we have considered. These materials exhibit yield points, serrated stress-strain curves, and strain aging effects[78,79] and do not strain harden even at temperatures as low as $0.29T_m$[80].

There is much additional work necessary in order to understand better the

influence of microstructure on the threshold stress in dilute dispersion hardened materials. It would seem to us that our relation, equation (7), may help to separate the influence of subgrain size and threshold stress on the creep rate. For example, an experiment of the following type may provide new useful information in elucidating better the creep properties of O.D.S. alloys. T-D nickel could be warm processed (400-700°C) to large strains at several strain rates. The subgrain structure could then be characterized. Creep rate stress relations determined for these differently processed materials could be plotted in a manner to eliminate subgrain-size as a variable. That is, plots of logarithm $\dot{\varepsilon}/D\lambda^3$ versus logarithm σ/E could be made which would permit determination of the threshold stress for each processing condition. The end objective, then, would be to determine the microstructural feature that contributes to the magnitude of the threshold stress observed.

SUMMARY AND CONCLUSIONS

The creep of oxide dispersion strengthened alloys is shown to follow many of the characteristics that describe the creep behavior of pure metals and many solid solution alloys. Such O.D.S. alloys are characterized by creep curves or stress-strain curves that exhibit negligible strain hardening. Thus, one can consider that these materials deform plastically under constant structure. It is shown that many O.D.S. alloys follow the same creep relation as developed for the creep of pure metals at constant structure. This equation is given by,

$$\dot{\varepsilon} = K \left(\frac{\lambda}{b}\right)^3 \frac{D_{eff}}{b^2} \left(\frac{\sigma}{E}\right)^n \qquad (6)$$

where $\dot{\varepsilon}$ is the creep rate, λ is the subgrain size, D_{eff} is the effective diffusion coefficient, σ is the creep stress, E is the dynamic unrelaxed average Young's modulus, n is the stress exponent equal to eight, b is the Burgers vector and K is a function of stacking fault energy, equal to about 10^9 for high stacking fault energy materials. This equation is shown to predict the creep behavior of many

O.D. S. alloys inasmuch as the stress exponent of such materials is usually high, and often nearly equal to eight (typically 7 to 10). The strength of O.D.S. alloys is attributed to the small value of λ in equation (6), that is, to the small subgrain size that is generally present in such materials and stabilized by the presence of the oxide particles.

A second feature of the O.D.S. alloys is that they oftentimes exhibit a threshold stress below which creep apparently does not take place. The microstructural feature that controls the threshold stress is not well understood but is often related theoretically to the Orowan bowing stress and phenomenologically to the G.A.R. (grain aspect ratio). When a threshold stress exists, equation (6) can still predict the behavior of such O.D.S. alloys by the following relation,

$$\dot{\epsilon} = k \left(\frac{\lambda}{b}\right)^3 \frac{D_{eff}}{b^2} \left(\frac{\sigma-\sigma_o}{E}\right)^8 \qquad (7)$$

where $\frac{\sigma_o}{E}$ is the modulus compensated threshold stress.

At high stresses, the fine subgrain structure that is initially present in the O.D.S. alloy may be coarser than the equilibrium subgrain size expected for the matrix of the alloy. The creep rate in this range is then controlled by the normal creep relation observed for metals where the subgrain size is a variable with stress. That is, the creep rate of O.D.S. alloys at high stress is expected to follow the behavior of the matrix material devoid of oxide particles. In this range strain hardening is expected to dominate the deformation process as subgrains are refined with deformation leading to an increase in creep resistance. This is verified for the case of our coarse grain T. D. Nichrome (Figure 16).

The major conclusion one must deduce from the analyses of the O.D.S. alloys done here is that such materials are controlled principally by the creep behavior of the matrix material. Diffusion controlled slip creep is well established

as the rate-controlling process in pure metals and many solid solutions at intermediate stresses and it is concluded that O.D.S. alloys are also controlled by the same mechanism. It is likely that the glide and climb of edge dislocations, associated with the subgrain structure as barriers, is the specific rate-controlling step.

ACKNOWLEDGEMENTS

This program was sponsored by the Lewis Research Center of NASA and monitored by Dr. J. Daniel Whittenberger. The authors are very appreciative of the wholehearted cooperation and continuous encouragement given by Dr. Whittenberger. His active participation in the program helped to optimize our contribution in the field of O.D.S. alloys. We also wish to thank Professor William D. Nix, Dr. Jurgen Hausselt and Dr. Steven L. Robinson for many discussions on the properties and structure of O.D.S. alloys; we also acknowledge Dr. Robinson's experimental work in the early phase of this program. The authors give thanks to Mr. Charles Blankenship of the NASA Lewis Research Center for his support of this program.

APPENDIX

It was not our intention to make an exhaustive survey of all the elevated temperature creep data on oxide dispersion strengthened materials. Rather, we simply intended to add additional information to that gathered earlier by Bird, Mukherjee and Dorn[1]. These authors showed that a number of O.D.S. materials exhibited a stress exponent of seven to eight citing principally the data of Wilcox and Clauer[14,15] on nickel-thoria and Ni-Cr-thoria alloys.

In our attempt to find further evidence for the high stress exponents observed in nickel base alloys, we uncovered the data plotted in Figure 8 which illustrates the creep behavior of several O.D.S. alloys including Cu-2% Al_2O_3, αU-3.5% Al_2O_3, Mg-0.5% MgO, Al-6% Al_2O_3 and Ni-3% Al_2O_3. The data indeed, give further evidence for a power law relation for creep of O.D.S. alloys and the data for individual materials fall on a common line when plotted as logarithm of $\dot{\varepsilon}/D_{eff}$ versus logarithm of σ/E. In the following section, we show the importance of the modulus correction factor in obtaining activation energies that can be related to diffusion activation energies.

In Figures A1 to A4 the raw data for each material (with the exception of αU-3.5% Al_2O_3 where data at only one temperature was reported) are plotted as logarithm $\dot{\varepsilon}$ versus logarithm σ. The activation energies, in kjoules per mole, are given in parentheses for each material. As noted previously for fine grain T.D. nichrome, these activation energies, especially at temperatures above 0.6 T_m, are higher than those for lattice self-diffusion.

In Figures A5 to A8, the data for each O.D.S. alloy are replotted as logarithm $\dot{\varepsilon}$ versus logarithm σ/E. These plots reveal activation energies for creep which, on the average, are equal to the activation energy for lattice self-diffusion, when data above 0.6 T_m are considered.

When data below 0.6 T_m are considered, the activation energy is less than that for lattice self-diffusion. The Mg-0.5% MgO data (Figure A6) represents a good example showing this trend. The activation energy for creep diminishes with decreasing temperature below 0.6 T_m and at the lowest temperatures of testing is equal to about 95 kj. per mole. This value is about two thirds of that for lattice self-diffusion (135 kj. per mole)[49] and can be associated with that for dislocation pipe diffusion. This trend in activation energy variation with temperature is similar to the trend noted previously for pure tungsten[22], pure aluminum[56], pure zinc[57] and pure copper[55] and suggests that the Mg-MgO data can be analyzed by means of an effective diffusion coefficient which incorporates the contribution of lattice and dislocation core diffusion to the overall diffusion process. Following the method used to analyze the creep data for pure aluminum[56], D_{eff} is given by,

$$D_{eff} = D_L + D_d \, 200 \left(\frac{\sigma}{E}\right)^2 ,$$

where D_L is the lattice diffusion coefficient and D_d is the diffusion coefficient in the core of the dislocation. The value of D_L is given by 1.25 $\exp -Q_L/RT$ cm^2/sec where Q_L = 135 kjoules per mole[49]. The value of D_d was chosen as 0.5 $\exp -Q_d/RT$ cm^2/sec where Q_d was assumed equal to 92 kjoules per mole [both $(D_o)_d$ and Q_d are reasonable values based on dislocation pipe diffusion studies in other metal systems][81]. Thus, the effective diffusion coefficient chosen for analyzing the Mg-0.5% MgO data, and used in Figure 8, was selected as

$$D_{eff} = 1.25 \exp^{-135/RT} + 100 \exp^{-92/RT} \left(\frac{\sigma}{E}\right)^2$$

where R is in units of kjoules per mole.

The resulting correlation shown in Figure 8 for the Mg-0.5% MgO data is impressive. A straight line, with n = 9, is obtained with excellent correlation of all the data from 0.46 to 0.90 T_m. It is of interest to note that the steep slope noted in Figure A6 at the two lowest temperatures (n equals about eleven) is decreased to n = 9 in Figure 8. This is because of the contribution of dislocation pipe diffusion to the overall diffusion process through the term $(\frac{\sigma}{E})^2$ which describes the increase in dislocation density with stress.

References

1. J. E. Bird, A. K. Mukherjee and J. E. Dorn, Int. Conf. Quantitative Relation Between Properties and Microstructure, Haifa, Israel, 1969, p. 255.

2. J. Weertman, Trans. ASM, vol. 61, p. 681.

3. O. D. Sherby and P. M. Burke, Prog. Mat. Sci., 1968, vol. 13, p. 325.

4. O. D. Sherby, R. H. Klundt and A. K. Miller, Met. Trans., 1977, vol. 8A, p. 843.

5. J. W. Edington, K. N. Melton and C. P. Cutler, Prog. Mats. Sci., 1976, vol. 21, p. 61.

6. B. A. Wilcox and A. H. Clauer, Trans. AIME, 1966, vol. 236, p. 570.

7. B. A. Wilcox, A. H. Clauer and W. S. McCain, Trans. AIME, 1967, vol. 239, p. 1791.

8. C. C. Meyers, J. C. Shyne and O. D. Sherby, J. A. Inst. Met., 1963, vol. 8, p. 171.

9. M. Malu and J. K. Tien, Acta Met., 1974, vol. 22, p. 145.

10. S. L. Robinson and O. D. Sherby, Conference and Materials Science Symposium, Annual AIME Meeting, Journal of Metals Abstract, Oct. 21, 1974, Detroit, Michigan.

11. R. W. Lund and W. D. Nix, Met. Trans., 1975, vol. 6A, p. 1329.

12. M. Malu and J. K. Tien, Scripta Met., 1975, vol. 9, p. 1117.

13. C. R. Barrett, A. J. Ardell and O. D. Sherby, Trans. AIME, 1964, vol. 230, p.200.

14. A. H. Clauer and B. A. Wilcox, Metal Sci. J., 1967, vol. 1, p. 86.

15. B. A. Wilcox and A. H. Clauer, Metal Sci. J., 1969, vol. 3, p. 26.

16. R. W. Lund and W. D. Nix, Acta Met., 1976, vol. 24, p. 469.

17. C. R. Barrett, Trans. AIME, 1967, vol. 239, p. 1726.

18. P. W. Davies, G. Nelmes, K. R. Williams and B. Wilshire, Metal Sci. J., 1973, vol. 7, p. 87.

19. K. R. Williams and B. Wilshire, Metal Sci. J., 1973, vol. 7, p. 176.

20. J. D. Parker and B. Wilshire, Metal Sci. J., 1975, vol. 9, p. 248.

21. R. S. W. Shewfelt and L. M. Brown, Phil. Mag., 1974, vol. 30, p. 1135.

22. S. L. Robinson and O. D. Sherby, Acta Met., 1969, vol. 17, p. 109.

23. W. J. Evans and G. F. Harrison, Metal Sci., 1976, vol. 10, p. 307.

24. R. Lagneborg and B. Bergman, Metal Sci., 1976, vol. 10, p. 20.

25. G. M. Pharr and W. D. Nix, Scripta Met., 1976, vol. 10, p. 1007.

26. J. H. Hausselt and W. D. Nix, Acta Met., 1977, vol. 25, p. 1491.

27. J. D. Whittenberger, Met. Trans., 1976, vol. 7A, p. 611.

28. K. Monma, H. Suto and H. Oikawa, J. Japan Inst. Metals, 1964, vol. 28, p. 188.

29. D.M.I.C. Technical Note, "TD Nickel Chromium, A Report on Currently Available Information and Data", November 2, 1967. Also given in reference 16.

30. P. G. Bailey, and R. E. Kutchera, Technical Report, AFML-TR-73-294.

31. W. Boas and F. K. Mackenzie, "Progress in Metal Physics" vol. 2, Ed. by Bruce Chalmers, 1950.

32. J. L. Lytton, Ph.D. Thesis, Stanford University, Stanford Calif., 1962.

33. J. D. Whittenberger, Met. Trans., 1977, vol. 8A, p. 1155.

34. P. G. Bailey, NASA, CR-135269, 1977.

35. C. R. Barrett, J. L. Lytton and O. D. Sherby, Trans. AIME, 1967, vol. 239, p. 170.

36. J. L. Lytton, C. R. Barrett and O. D. Sherby, Trans. AIME, 1965, vol. 233, p. 1389.

37. P. Shahinian and M. R. Achter, Trans. ASM, 1959, vol. 51, p. 244.

38. K. Monma, H. Suto and H. Oikawa, J. Japan Inst. Metals, 1964, vol. 28, p. 253.

39. D. Sidey and B. Wilshire, Metal Sci. J., 1969, vol. 3, p. 56.

40. R. D. Kane and L. J. Ebert, Met. Trans., 1976, vol. 7A, p. 133.

41. B. A. Wilcox and A. H. Clauer, Acta Met., 1972, vol. 20, p. 743.

42. H. Suto, T. Uno and G. Nakamura, J. Japan Inst. Metals, 1969, vol. 33, p. 1417.

43. A. S. Bufferd, K. M. Zwilsky and N. J. Grant, Trans. ASM, 1963, vol. 56, p. 508.

44. K. Milicka, J. Cadek and P. Rys, Acta Met., 1970, vol. 18, p. 1071.

45. H. Hsu, C. Y. Chen, S. C. Yang and O. D. Sherby, J. Taiwan Mat. Sci., 1974, vol. 6, p. 167.

46. S. Takahashi, K. Iida and M. Adachi, Trans. Natl. Res. Inst. Metals, 1964, vol. 6, p. 29.

47. A. Kuper, H. Letaw, L. Slifkin, E. Sonder and C. T. Tomizuka, Phys. Rev., 1955, vol. 98, p. 1870.

48. Y. Adda and A. Kirianenko, J. Nucl. Mat., 1962, vol. 6, p. 130.

49. P. G. Shewmon, Trans. AIME, 1956, vol. 206, p. 918.

50. T. S. Lundy and J. F. Murdock, J. Appl. Phys. 1962, vol. 33, p. 1671.

51. W. R. Upthegrove and M. J. Sinnott, Trans. ASM, 1958, vol. 50, p. 1031.

52. W. Koster, Z. Metallk, 1940, vol. 32, p. 160.

53. P. E. Armstrong and H. L. Brown, Trans. AIME, 1964, vol. 230, p. 962.

54. M. E. Fine, Rev. Sci. Instruments, 1957, vol. 28, p. 643.

55. C. R. Barrett and O. D. Sherby, Trans. AIME, 1964, vol. 230, p. 1322.

56. O. D. Sherby and C. M. Young, Rate Processes in Plastic Deformation of Materials, Proceedings from the John E. Dorn Symposium, American Society for Metals, 1975, p. 497.

57. G. R. Edwards. T. R. McNelley and O. D. Sherby, Scripta Met., 1974, vol. 8, p. 475.

58. Shu-en Hsu, The Mechanical Behavior of Cadmium Base Composites, Ph. D. Dissertation, Stanford University, Stanford, California, June 1972.

59. R. J. Schafer, M. Quatinetz and J. W. Weeton, Trans. AIME, 1961, vol. 221, p. 1099.

60. Glidden Metals, Brochure on Glidcop, No. 04177, 1973.

61. F. C. Monkman and N. J. Grant, Proc. ASTM, 1956, vol. 56, p. 593.

62. C. M. Young, S. L. Robinson and O. D. Sherby, Acta Met., 1975, vol. 23, p. 633.

63. A. M. Gervais, J. T. Norton and N. J. Grant, Trans. AIME, 1953, vol. 197, p. 1166.

64. R. Horiuchi and M. Otsuka, Trans. Jap. Inst. Metals, 1972, vol. 13, p. 284.

65. C. N. Ahlquist and W. D. Nix, Scripta Met., 1969, vol. 3, p. 679.

66. O. D. Sherby, R. E. Frenkel, J. Nadeau and J. E. Dorn, Trans. AIME, 1954, vol. 200, p. 275.

67. L. Raymond, and J. E. Dorn, Trans AIME, 1964, vol. 230, p. 560.

68. A. H. Clauer, Third Nordic High Temperature Symposium, 1972, page 167, Figure 9).

69. P. F. Sikora and Max Quatinetz, NASA TMX-2548, April 1972.

70. J. J. Petrovic and L. J. Ebert, Met. Trans, 1973, vol. 4, p. 1301.

71. R. W. Guard, in Creep and Recovery, American Society for Metals, Ohio, 1957, p. 251.

72. A. W. Thompson, Acta Met., 1975, vol. 23, p. 1337.

73. J. H. Hausselt and W. D. Nix, Acta Met., 1977, vol. 25, p. 595.

74. M. F. Ashby, Phil. Mag., 21, (170), 1970, p. 399.

75. R. W. Fraser, B. Meddings, D. J. I. Evans and V. N. Machiw, Modern Development in Powder Metallurgy, edited by H. H. Hausner, p. 87, Plenum Press (1966).

76. B. B. Burton, Metal Sci. J., 1971, vol. 5, p. 11.

77. G. R. Edwards, T. R. McNelley and O. D. Sherby, Phil. Mag., 1975, vol. 32, p. 1245.

78. T. R. McNelley, G. R. Edwards, D. Francois, W. H. McCarthy, J. C. Shyne, and O. D. Sherby, Met. Trans., 1972, vol. 3, p. 1316.

79. I. C. Huseby, S. E. Hsu, T. R. McNelley, G. R. Edwards, D. Francois, J. C. Shyne and O. D. Sherby, Met. Trans., 1975, vol. 6A, p. 2005.

80. T. R. McNelley, G. R. Edwards and O. D. Sherby, Acta Met., 1977, vol. 25 p. 117.

81. N. A. Gjostein, Diffusion, ASM, Metals Park, Ohio, 1972, p. 257.

Table I

Tabulation of High Temperature Compression Data on Fine Grained T-D Nichrome

Orientation	Temp.	$\dot{\varepsilon}(sec^{-1})$	$\frac{\dot{\varepsilon}}{D}(cm^{-2})$	σ(MPa)ksi	$\sigma/E(10^{-3})$
Longitudinal	900°C	$8x10^{-3}$	$2.9x10^{10}$	(204.8)29.7	1.2
		$1.5x10^{-4}$	$5.4x10^{8}$	(135.1)19.0	0.8
		$1.5x10^{-5}$	$5.4x10^{7}$	(118.6)17.2	0.7
	1000°C	$1.5x10^{-2}$	$5.4x10^{8}$	(173.7)25.2	1.08
		$1.5x10^{-4}$	$5.4x10^{7}$	(106.8)15.5	.67
		$1.5x10^{-5}$	$5.4x10^{6}$	(83.4)12.1	.52
	1100°C	$8x10^{-3}$	$4x10^{8}$	(110.3)16.	.77
		$7.6x10^{-4}$	$4x10^{7}$	(73.1)10.6	.51
		$7.4x10^{-5}$	$4x10^{6}$	(62.0) 9.0	.43
	1200°C	$1.5x10^{-5}$	$1.5x10^{5}$	(42.0) 6.1	.34
		$1.6x10^{-4}$	$1.6x10^{6}$	(52.4) 7.6	.43
		$1.6x10^{-3}$	$1.6x10^{7}$	(68.2) 9.9	.55
	1200°C	$1.6x10^{-5}$		(40.7) 5.9	.33
	900°C	$1.5x10^{-5}$	$5.4x10^{7}$	(113.8)16.5	.67
		$1.5x10^{-4}$	$5.4x10^{8}$	(150.0)21.7	.88
		$1.6x10^{-3}$	$5.5x10^{9}$	(191.0)27.7	1.13
	1000°C	$1.6x10^{-5}$	$5.8x10^{6}$	(95.5)13.8	.60
		$1.6x10^{-4}$	$5.8x10^{7}$	(112.7)16.35	.43
		$1.8x10^{-3}$	$6.0x10^{8}$	(136.2)19.75	.85
Short Transverse	900°C	$9x10^{-3}$	$3.3x10^{10}$	(241.3)35.1	1.42
		$1.4x10^{-4}$	$5x10^{8}$	(138.0)20.0	.81
		$1.4x10^{-5}$	$5x10^{7}$	(120.0)17.4	.70
	900°C	$1.14x10^{-5}$	$5.1x10^{7}$	(103.0)14.9	6.07
		$5.87x10^{-5}$	$2.7x10^{8}$	(133.5)19.37	7.9
		$3.0x10^{-4}$	$1.36x10^{9}$	(162.6)23.59	9.6
		$1.27x10^{-3}$	$5.75x10^{9}$	(189.6)27.49	1.12
	1000°C	$8x10^{-3}$	$2.9x10^{9}$	(150.0)21.75	.93
		$1.5x10^{-4}$	$5.4x10^{7}$	(100.0)14.55	.63
		$1.6x10^{-5}$	$5.8x10^{6}$	(70.7)10.25	.44
		$2.9x10^{-4}$	$1.x10^{8}$	(114.5)16.6	.71
		$1.24x10^{-5}$	$4.5x10^{6}$	(71.7)10.3	.47
	1100°C	$8x10^{-3}$	$4x10^{8}$	(108.3)15.7	.75
		$8x10^{-5}$	$4x10^{6}$	(63.4) 9.2	.44
		$1.08x10^{-5}$	$6.5x10^{5}$	(58.0) 8.38	.42
		$6x10^{-5}$	$3x10^{6}$	(70.0)10.2	.5
		$3.14x10^{-4}$	$1.6x10^{7}$	(87.0)12.6	.62
		$1.2x10^{-3}$	$6x10^{7}$	(105.0)15.23	.75
	1200°C	$1.5x10^{-5}$	$1.4x10^{5}$	(34.1) 4.95	.28
		$1.6x10^{-4}$	$1.6x10^{6}$	(39.0) 5.6	.31
Long Transverse	900°C	$7x10^{-3}$	$2.6x10^{10}$	(244.0)35.35	1.42
		$1.4x10^{-4}$	$5x10^{8}$	(143.1)20.75	.84
		$1.4x10^{-5}$	$5x10^{7}$	(108.2)15.7	.64
	1000°C	$8x10^{-3}$	$2.9x10^{9}$	(154.4)22.4	.96
		$1.5x10^{-4}$	$5.4x10^{7}$	(102.4)14.85	.64
		$1.6x10^{-5}$	$5.8x10^{6}$	(70.0)10.15	.44
	1100°C	$8x10^{-3}$	$4x10^{8}$	(114.8)16.65	.80
		$8x10^{-4}$	$4x10^{7}$	(93.1)13.5	.65
		$8x10^{-5}$	$4x10^{6}$	(62.0) 9.0	.43

Table II

Tabulation of High Temperature Compression Data on Coarse grain T-D Nichrome

Orientation	Temp.	$\dot{\varepsilon}(sec^{-1})$	$\frac{\dot{\varepsilon}}{D}(cm^{-2})$	σ(MPa)ksi	$\sigma/E(10^{-3})$
Longitudinal	1000°C	4.83×10^{-3}	1.42×10^{9}	(171.7)24.9	1.07
		2.33×10^{-4}	6.9×10^{7}	(144.1)20.9	0.90
		2.37×10^{-5}	7×10^{6}	(134.5)19.5	0.84
	1000°C	4.8×10^{-3}	1.42×10^{9}	(177.2)25.7	1.10
		2.3×10^{-4}	6.8×10^{7}	(147.)21.32	0.92
		2.11×10^{-5}	6.25×10^{6}	(137.9)20.	0.86
	1100°C	5.71×10^{-3}	2.38×10^{8}	(134.5)19.50	0.94
		2.68×10^{-4}	1.12×10^{7}	(111.7)16.2	0.78
Transverse	1175°C	2.93×10^{-5}	3.86×10^{5}	(99.3)14.4	0.77
		1.18×10^{-5}	1.36×10^{5}	(97.2)14.1	0.76
	1100°C	4.75×10^{-3}	1.98×10^{8}	(137.2)19.9	0.96
		2.3×10^{-4}	9.6×10^{6}	(120.0)17.4	0.84
		9.25×10^{-6}	3.9×10^{5}	(110.0)15.9	0.76
	900°C	6.3×10^{-3}	1.84×10^{10}	(238.0)34.5	1.4
		1.24×10^{-3}	3.63×10^{9}	(203.4)29.5	1.2
		3.0×10^{-4}	8.8×10^{8}	(182.0)26.4	1.07
		3.0×10^{-5}	8.8×10^{7}	(162.0)23.5	0.96
		1.45×10^{-5}	4.3×10^{7}	(164.1)23.8	0.97
	900°C	2.6×10^{-4}	7.6×10^{8}	(182.7)26.5	1.08
		2.64×10^{-5}	7.7×10^{7}	(162.)23.5	0.96
	1000°C	6.26×10^{-3}	1.85×10^{9}	(180.0)26.1	1.12
		1.23×10^{-3}	3.64×10^{8}	(160.6)23.3	1.0
		2.93×10^{-4}	8.7×10^{7}	(144.8)21.0	.9
		2.98×10^{-5}	8.8×10^{6}	(134.4)18.5	.84
		1.21×10^{-5}	3.58×10^{6}	(131.7)19.1	.82

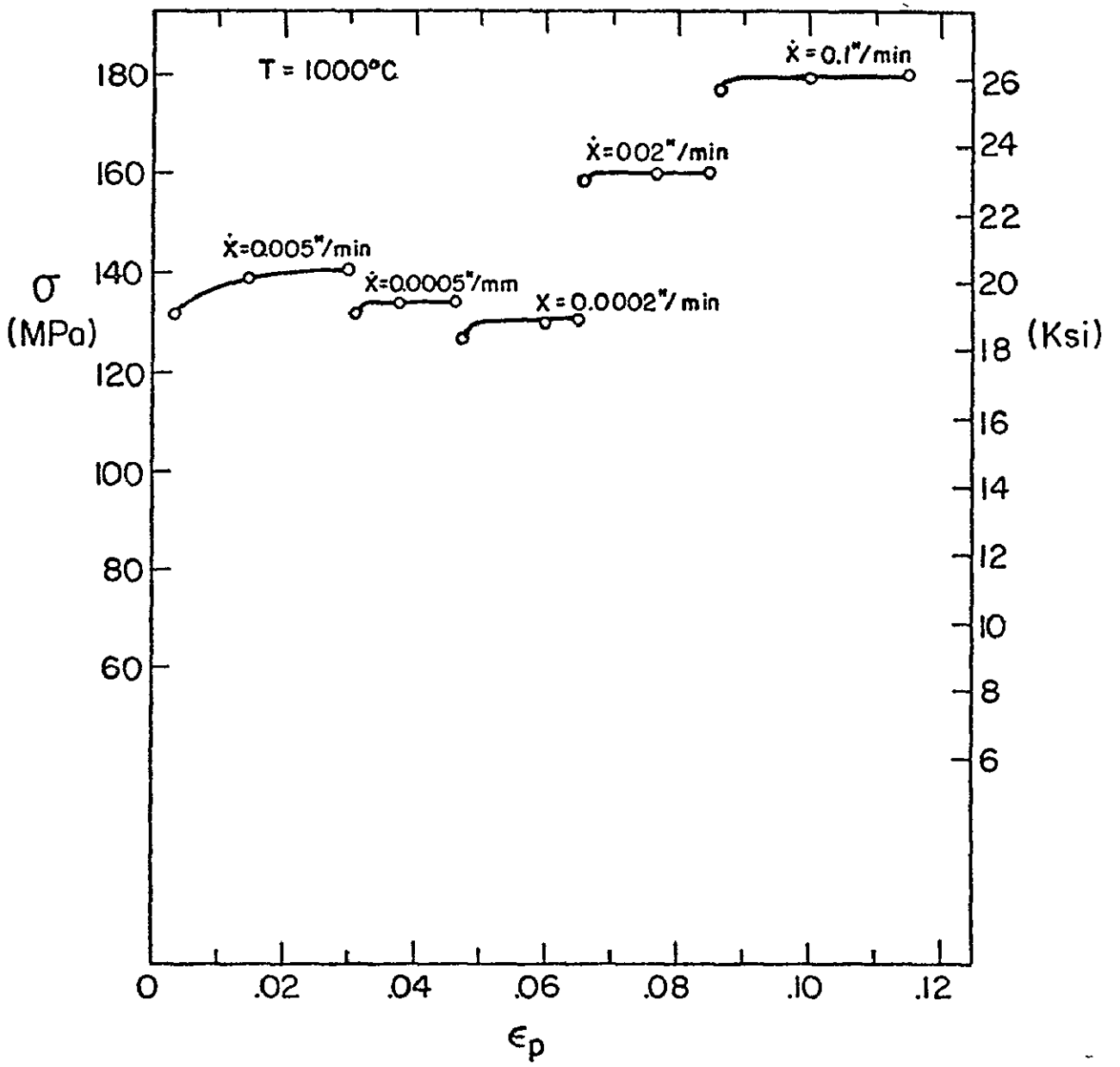

Figure 1. A typical change in cross head speed test for coarse grain size T-D Nichrome. Negligible strain hardening during straining was observed except in the first one to two percent strain.

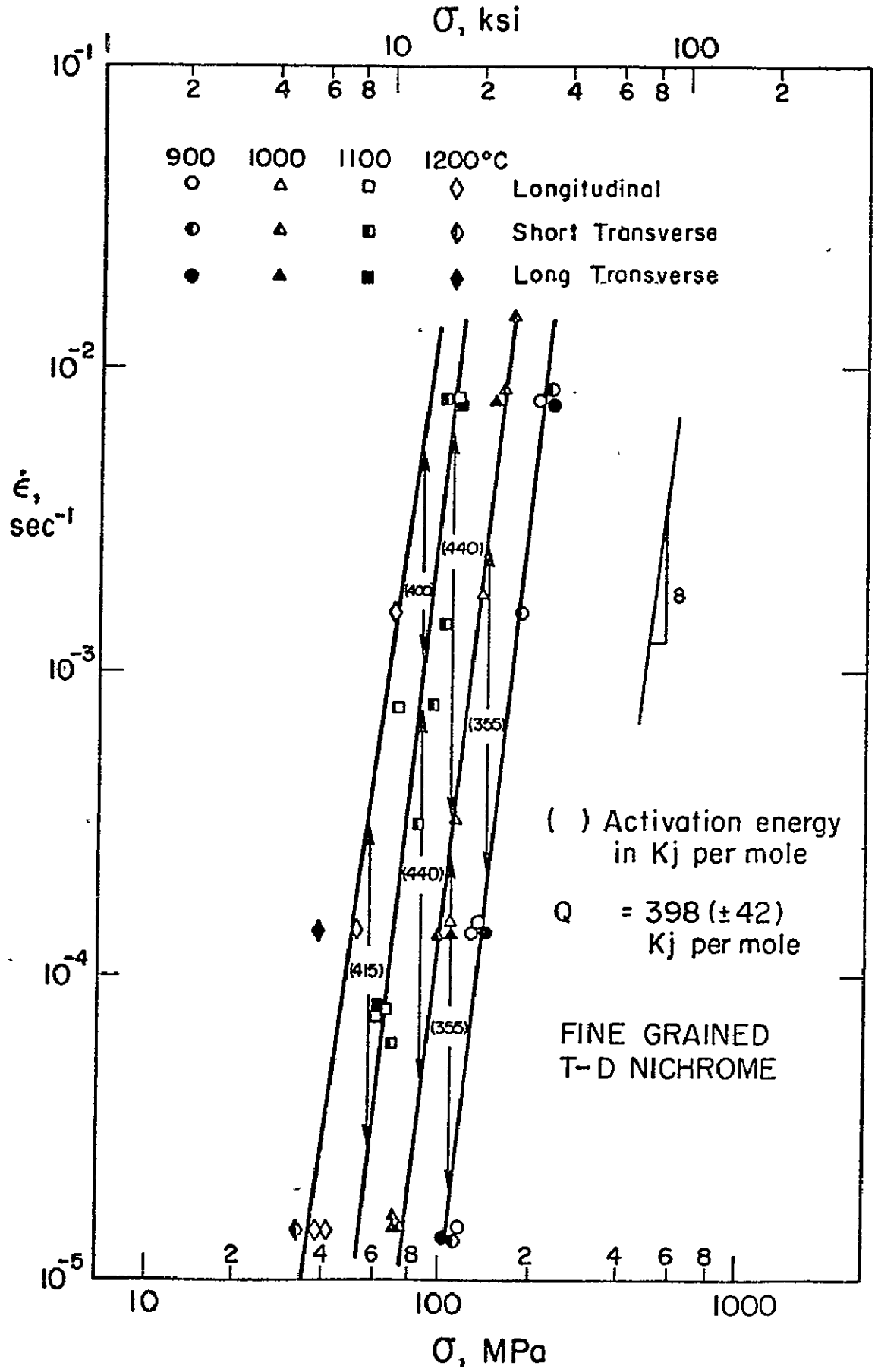

Figure 2. Logarithm of the flow stress, σ, is plotted against logarithm of the strain rate for fine grain T-D Nichrome at various temperatures. The average activation energy for creep noted (398 kjoules per mole) is considerably above that for lattice self-diffusion in Nichrome (285 kjoules per mole)[28].

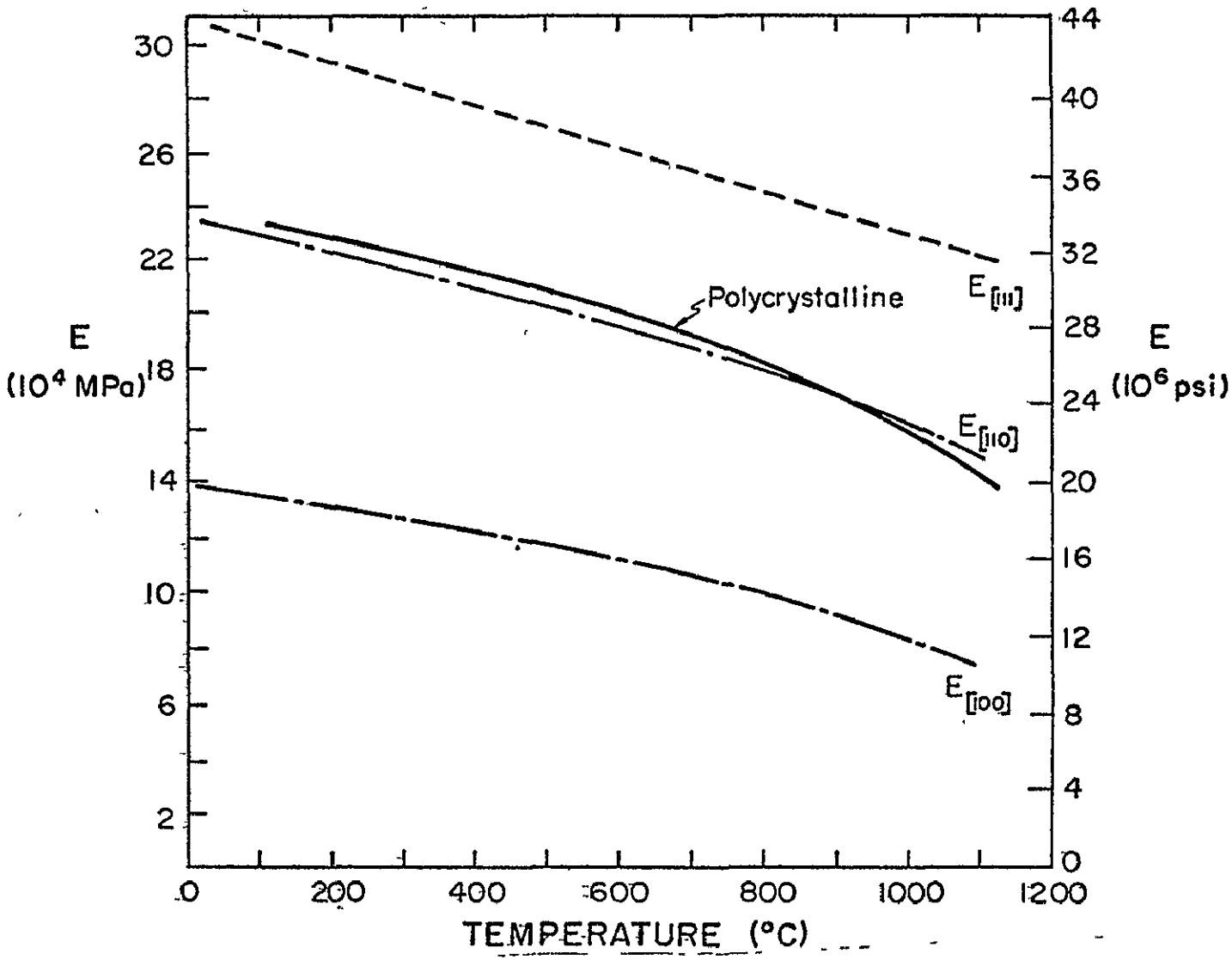

Figure 3. Dynamic modulus data for nichrome containing thoria particles as a function of temperature. The solid line is for polycrystalline T-D Nichrome[29]. The curves for E [110] and E [100] were obtained for directionally recrystallized D-S Nichrome[30]. The E [111] curve was calculated by us from the E [110] and E [100] data by standard relations[31]. The nearly perfect superposition of the curve for the polycrystalline sample with the E [110] curve indicates that the polycrystalline material is representative of a random polycrystalline aggregate[32].

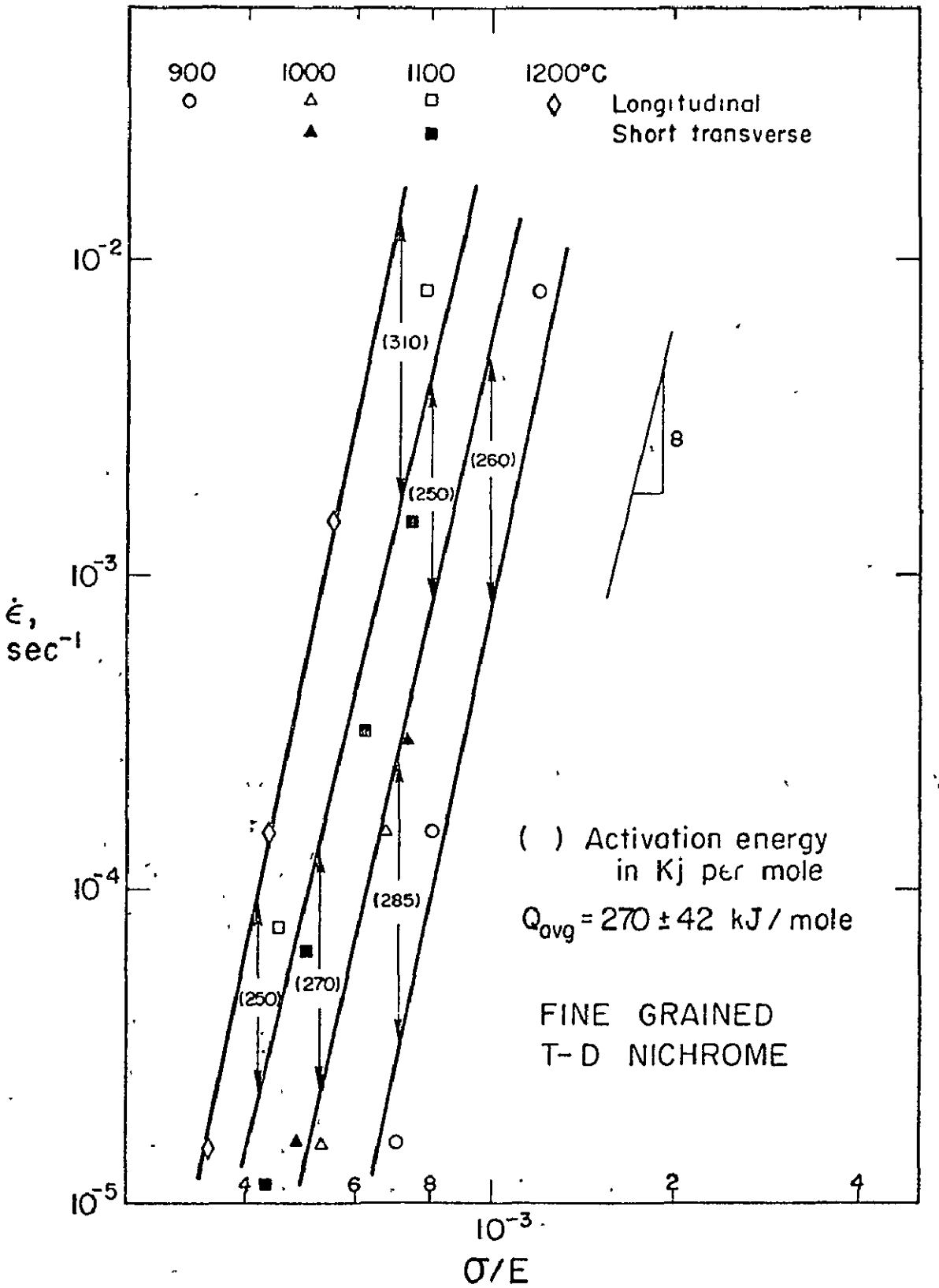

Figure 4. Logarithm of the modulus compensated flow stress is plotted against logarithm of the strain rate for fine grain T.D. Nichrome at various temperatures. The average activation energy for creep noted (270 kjoules per mole) is about equal to that for lattice self diffusion in nichrome (285 kjoules per mole)[28].

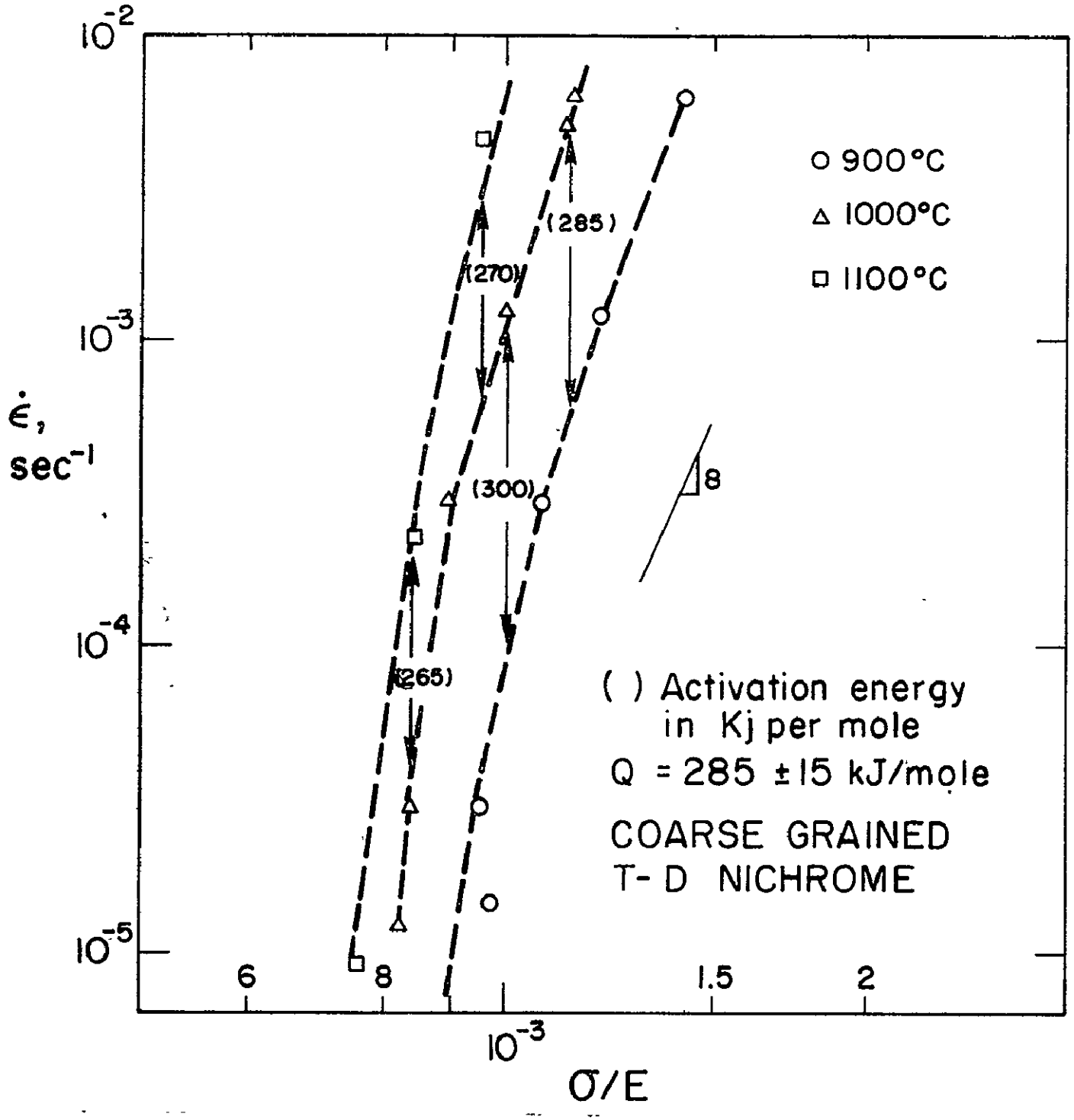

Figure 5. Logarithm of the modulus compensated flow stress is plotted against logarithm of the strain rate for coarse grain T. D. Nichrome at various temperatures. The average activation for creep noted (285 kjoules per mole) is equal to that for lattice self-diffusion in nichrome[28].

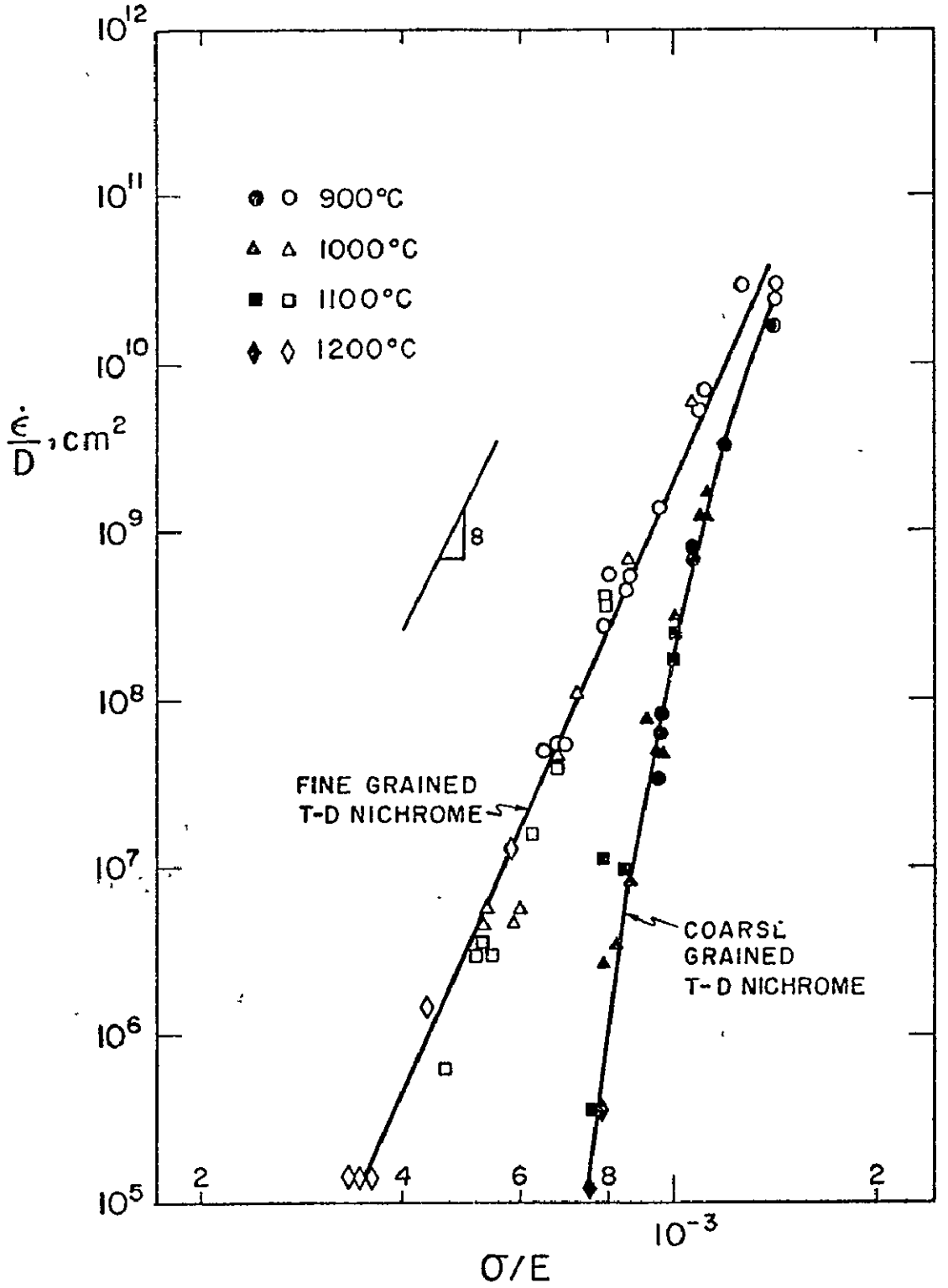

Figure 6. Logarithm of the modulus compensated flow stress is plotted against logarithm of the diffusion compensated strain rate for fine and coarse grain T. D. Nichrome. The coarse grain material is seen to be stronger than the fine grain material and appears to exhibit a threshold stress at low stresses. Diffusion data from reference 28 and modulus data from reference 29.

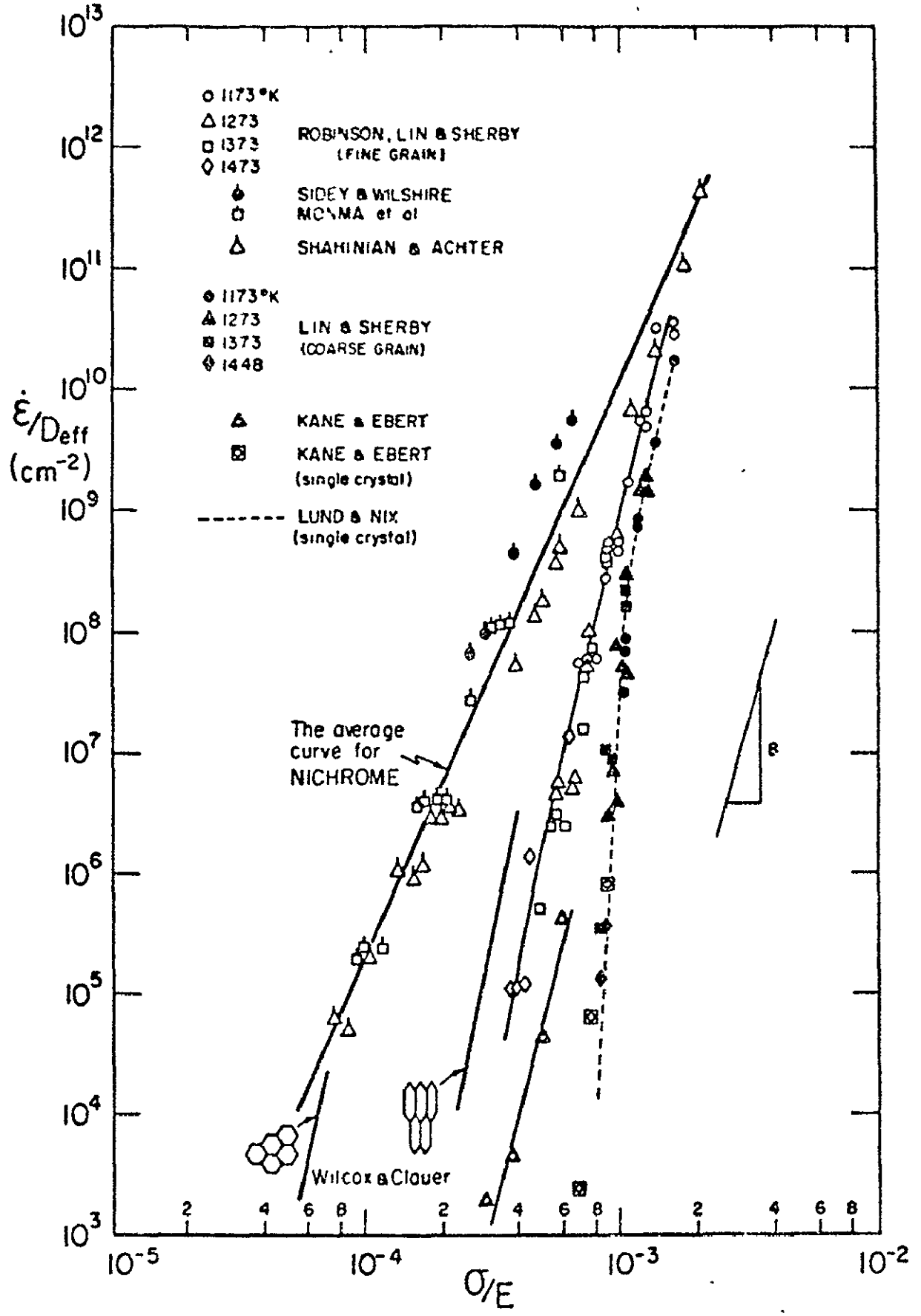

Figure 7. Creep data on T. D. Nichrome from various investigations are plotted as $\dot{\varepsilon}/D$ versus σ/E. The compression creep data of our investigation reveal that the coarse grain T. D. Nichrome is about equal in strength to the single crystalline material (T. D. Nichrome) studied by Lund and Nix[16] and Kane and Ebert[40]. The average creep behavior of nichrome studied by three separate investigators[37-39] is also shown for comparison.

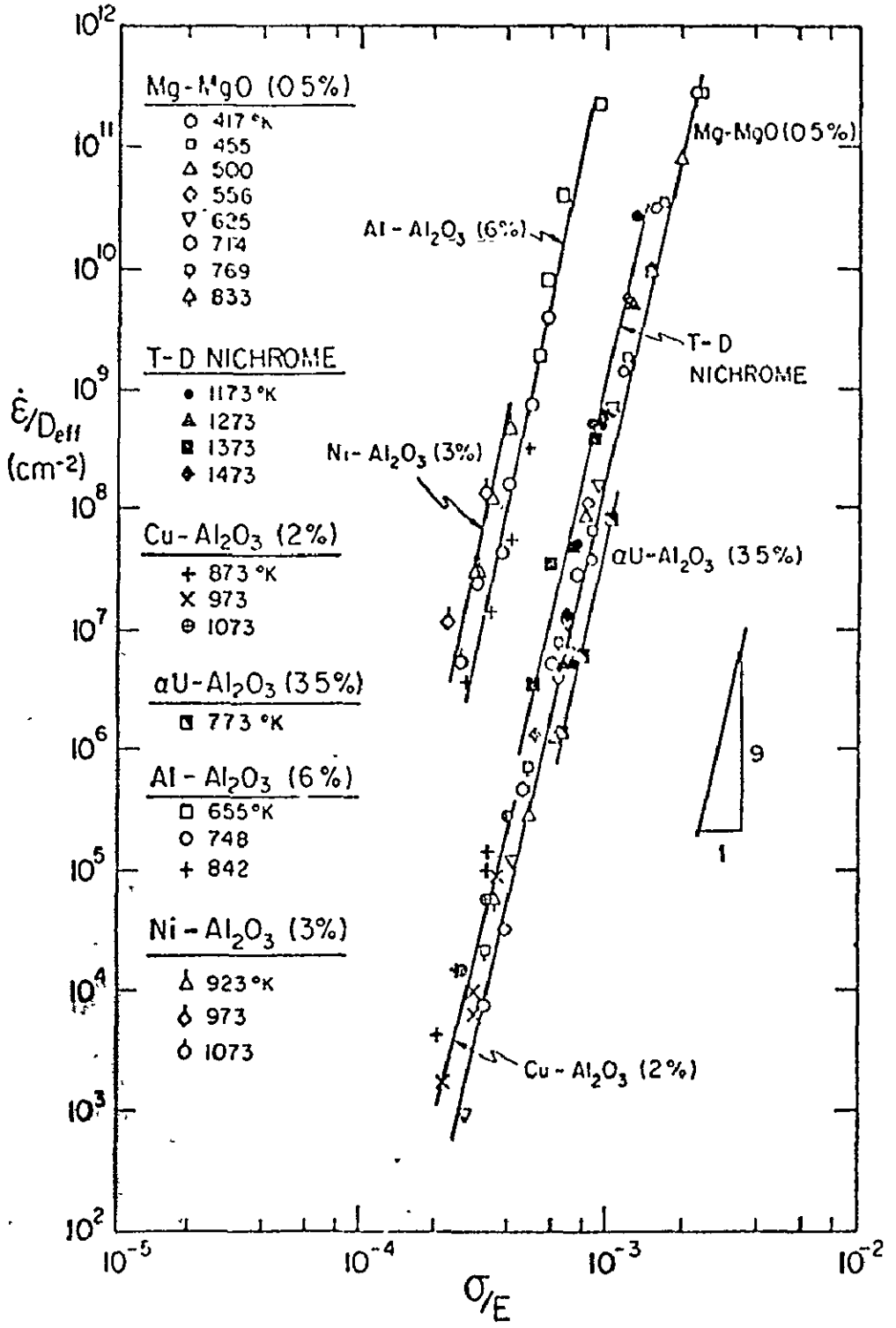

Figure 8. Comparison of the creep behavior of fine grain T. D. Nichrome of this investigation with other O.D.S alloys [42-46] by means of a diffusion compensated creep rate and a modulus compensated stress. The diffusion data were obtained from references 47-51 and the modulus data from references 52-54. The internal consistency of the above data suggests a common deformation mode for these O.D.S. materials which must incorporate the importance of elastic modulus and matrix diffusion on the creep process. The data given above also illustrates that the average stress exponent for creep is high and equal to about nine in contrast to a value of five for pure metals and many solid solution alloys.

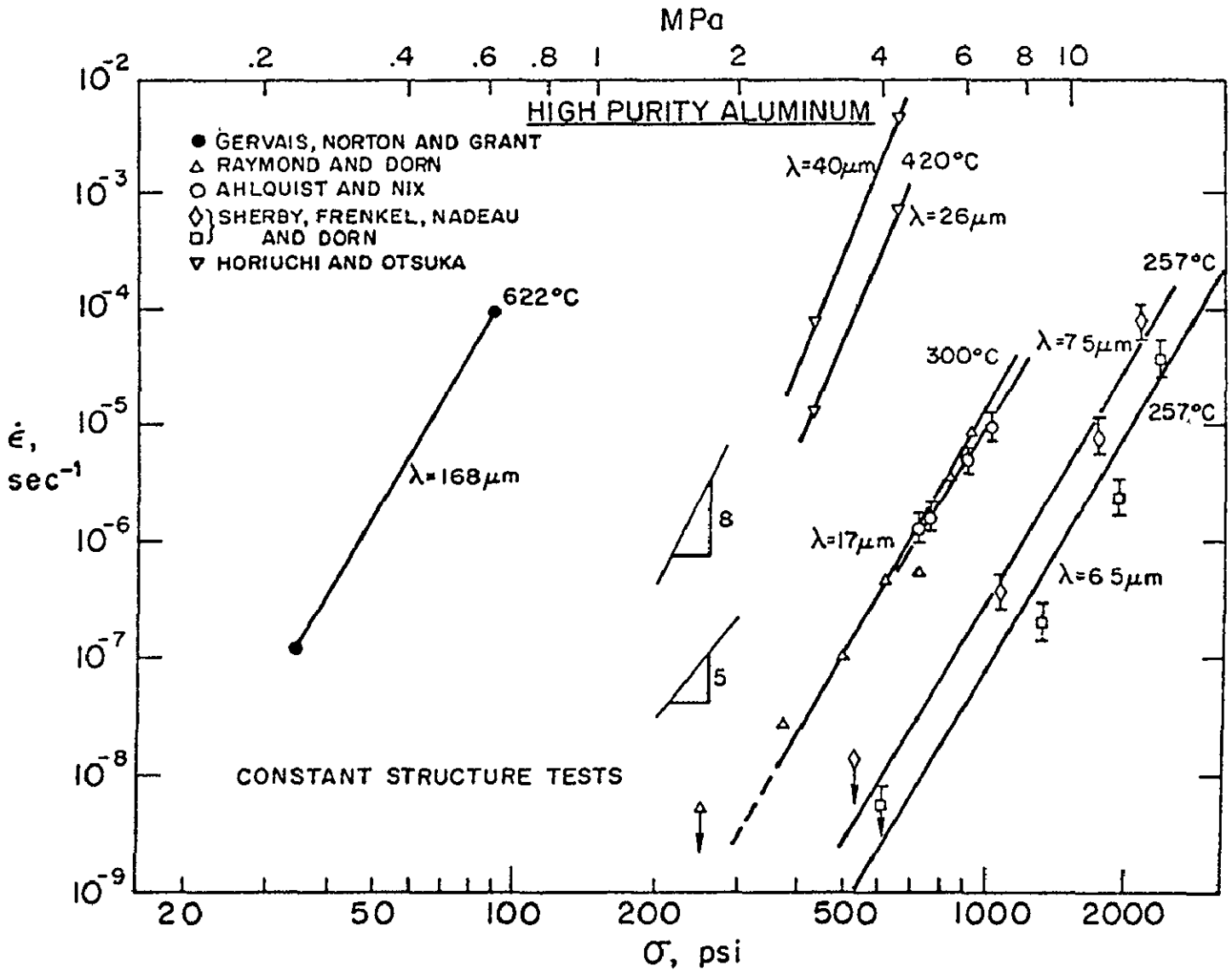

Figure 9. Constant structure creep tests[4] on high purity aluminum conducted by several investigators. The subgrain size for each test condition is shown in the graph and was obtained from reference 62. These constant structure creep tests reveal that the stress exponent is much above five and more nearly equal to about eight.

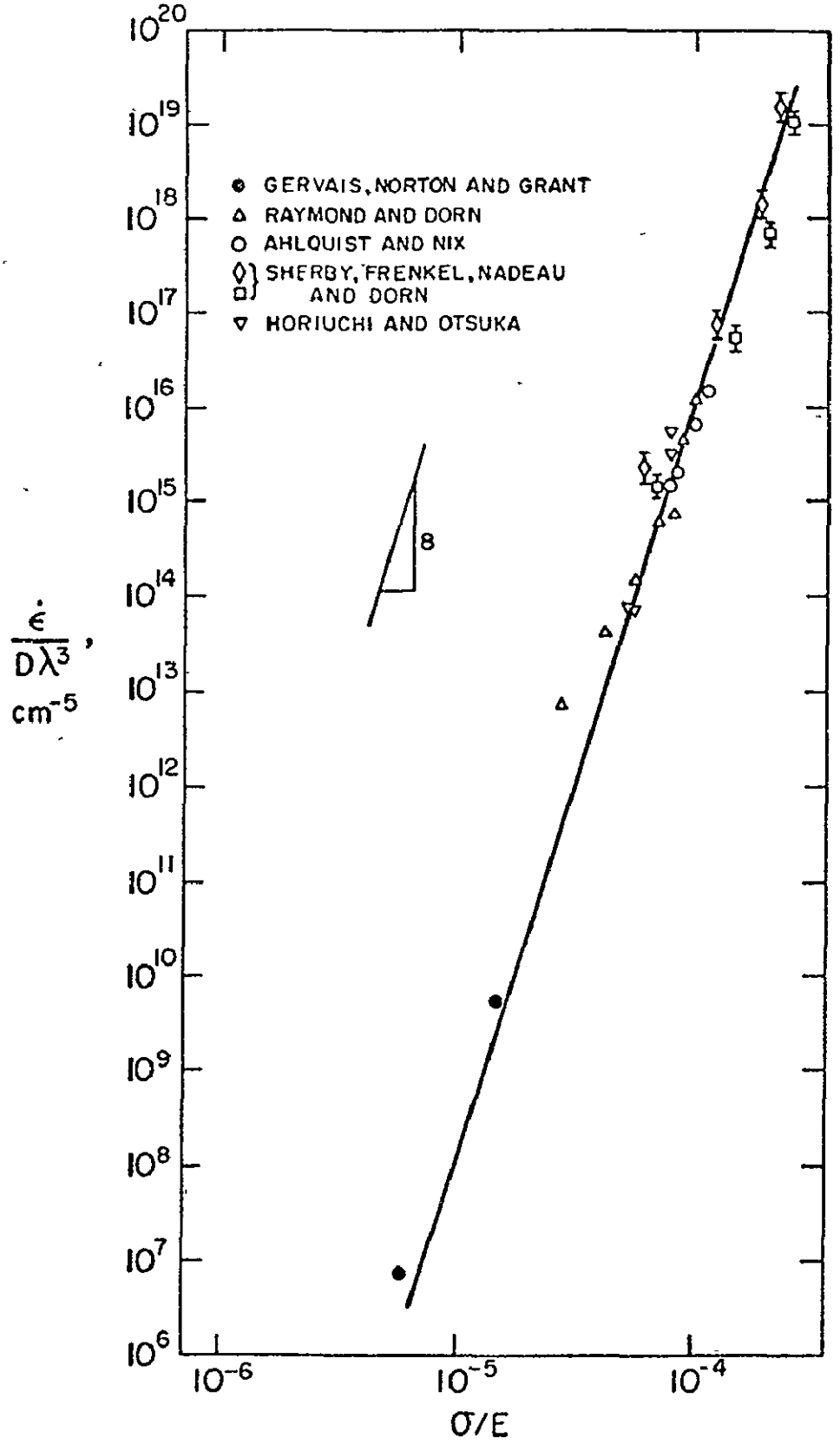

Figure 10 The constant structure creep tests of Figure 9 are replotted as logarithm $\dot{\epsilon}/D\lambda^3$ versus logarithm σ/E where λ is the subgrain size. The data superimpose on a common curve attesting to the proposal that $\dot{\epsilon} \alpha \lambda^3$ at constant diffusivity and modulus compensated stress. The slope of the above curve reveals that the stress exponent is about equal to eight.

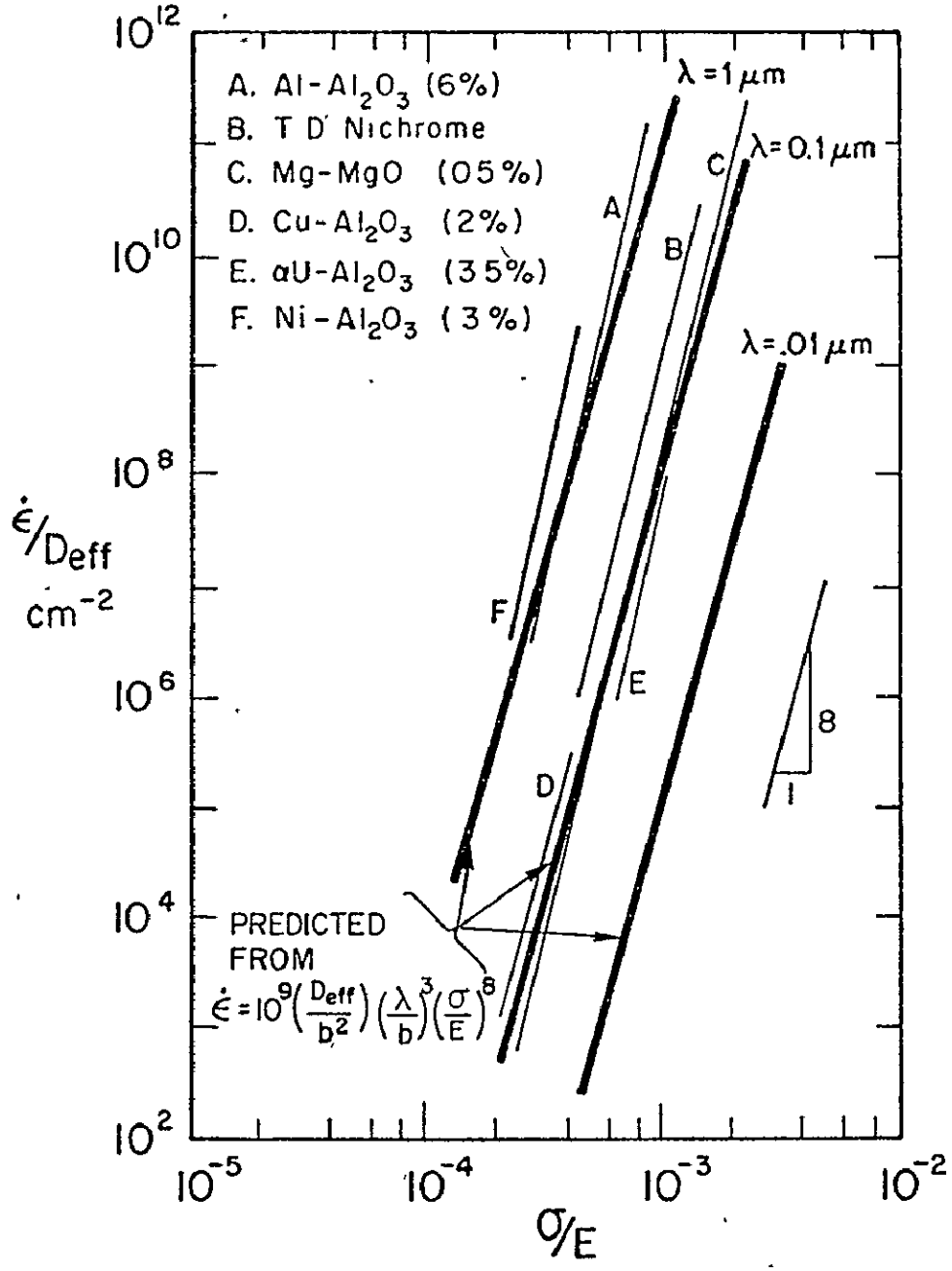

Figure 11. The creep data for various O.D.S alloys (taken from Figure 8) are compared with phenomenological equation (6) for three different subgrain sizes. The experimental curves fall within the subgrain size range of λ = 1μm to λ = 0.1μm. Such values of λ are typical of O.D.S. alloys, suggesting that equation (6) appropriately describ the influence of subgrains on the creep rate of many O.D.S. alloys.

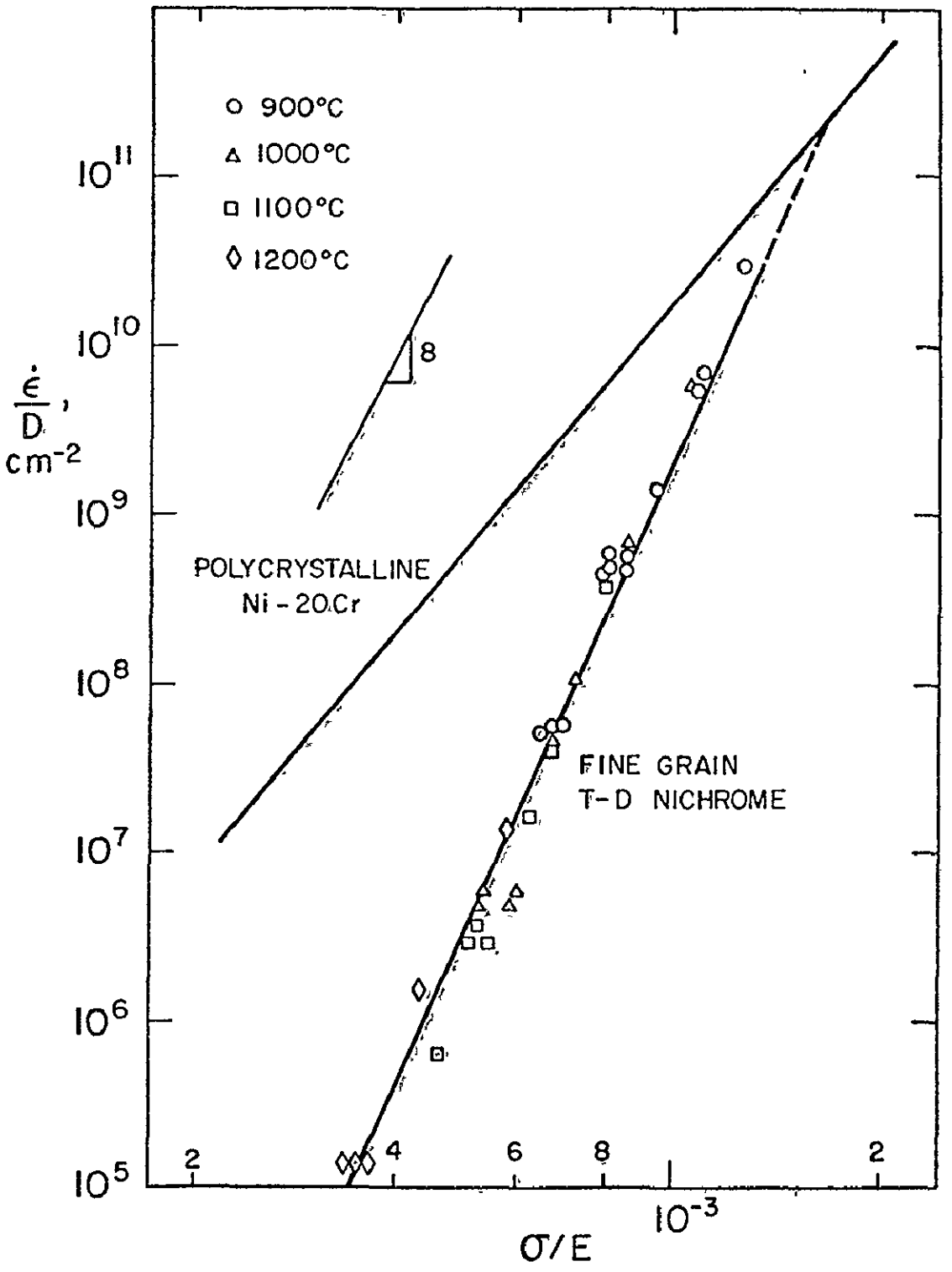

Figure 12. Comparison of the creep behavior of fine grain T.D. Nichrome with nichrome. The curves intersect at a value of $\sigma/E = 1.5 \times 10^{-3}$. At this modulus compensated stress, the subgrain size is calculated to be 0.5μm (see Figure 13).

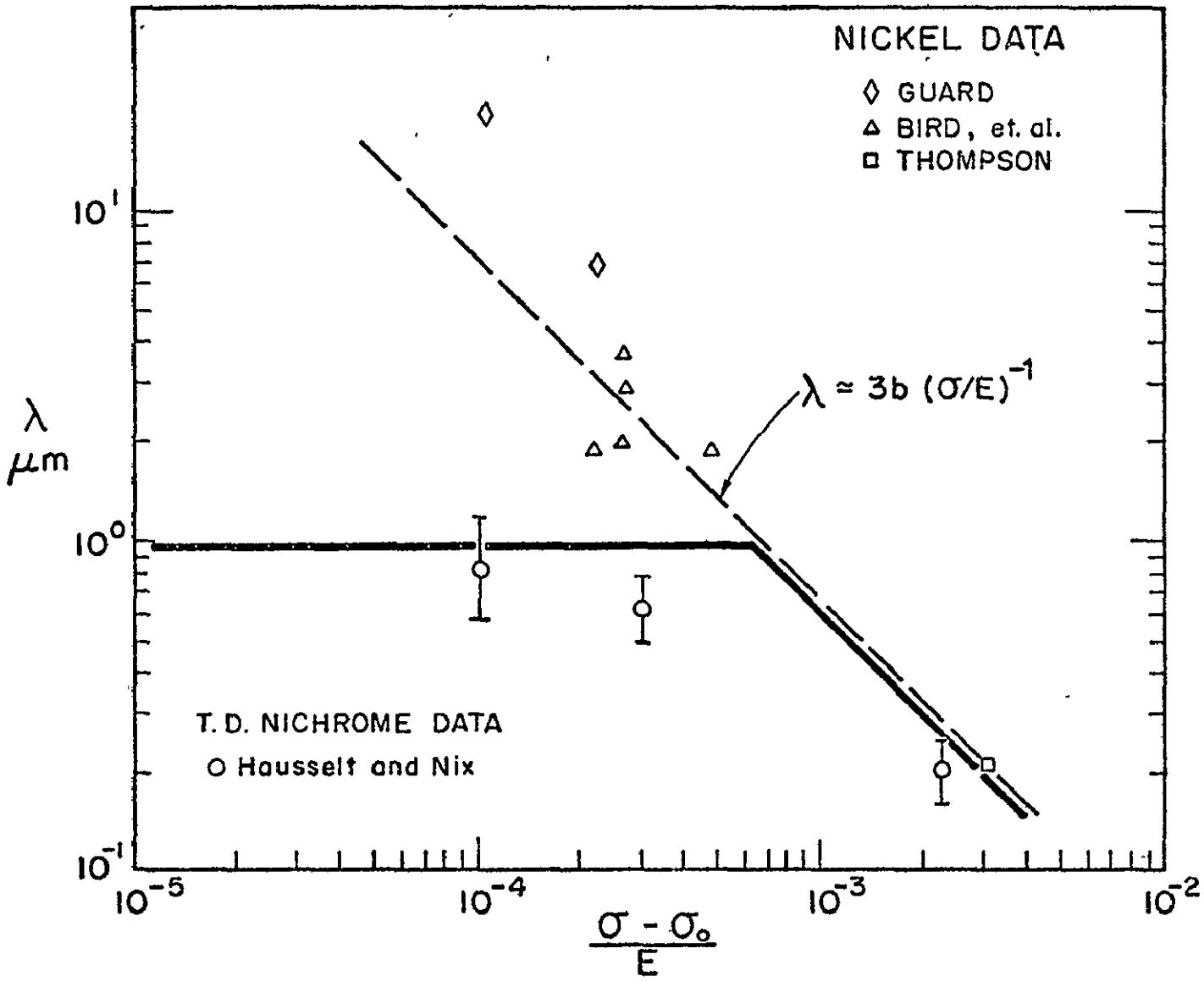

Figure 13. Logarithm of the subgrain size is plotted against logarithm of $\frac{\sigma-\sigma_o}{E}$ for coarse grain T.D. Nichrome[73] and for pure nickel[1,71,72]. The modulus compensated threshold stress σ_o/E is equal to 5.5×10^{-4} for coarse grain T.D. Nichrome and zero for the nickel data. The nickel data was used to estimate the subgrain size in nichrome as a function of σ/E.

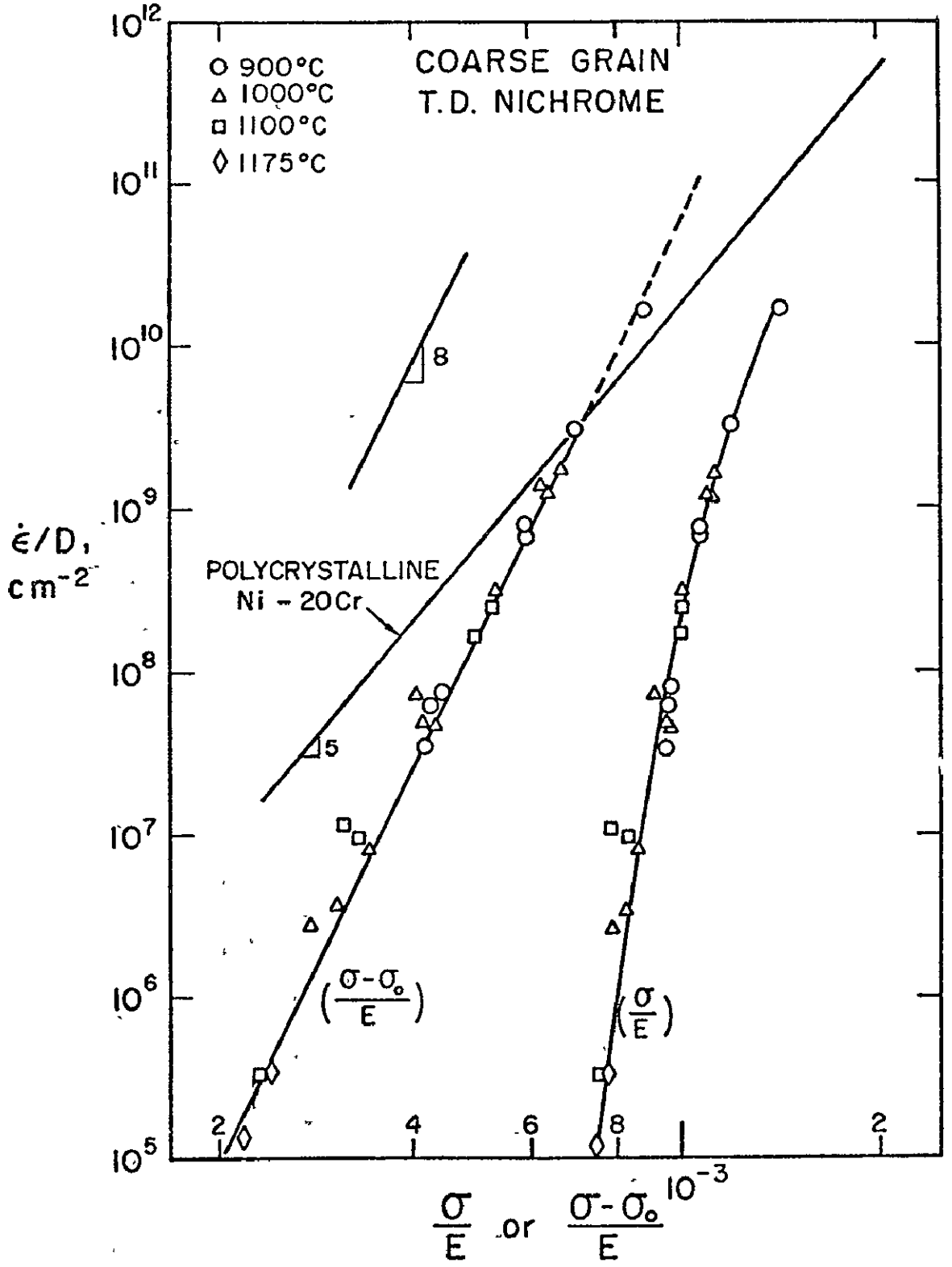

Figure 14. Comparison of the creep behavior of coarse grain T. D. Nichrome with nichrome. The coarse grain T. D. Nichrome is plotted as σ/E and as $\frac{\sigma-\sigma_o}{E}$ where $\frac{\sigma_o}{E}$ is the modulus-compensated threshold stress (equal to 5.5×10^{-4}). The latter plot yields a stress exponent of eight, and intersects the nichrome curve at $\frac{\sigma-\sigma_o}{E} = 7 \times 10^{-4}$. At this modulus compensated stress the subgrain size is 1.2μm (see Figure 13).

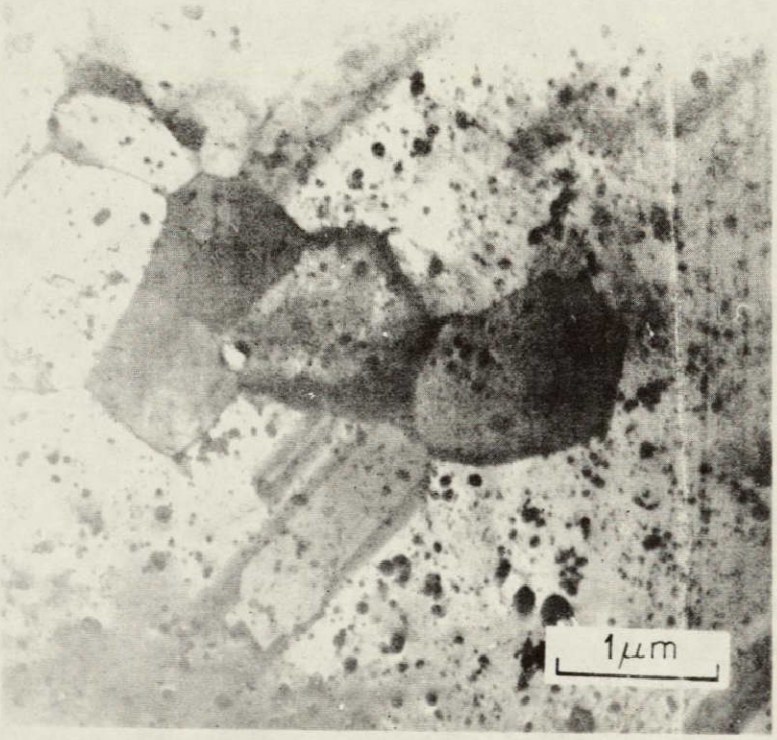

Figure 15. Transmission electron micrograph of as-received coarse grain T.D. Nichrome showing a region where subgrains were noted. The average subgrain size in such regions (representing about thirty percent of the material) was 1.2μm ± 0.2μm.

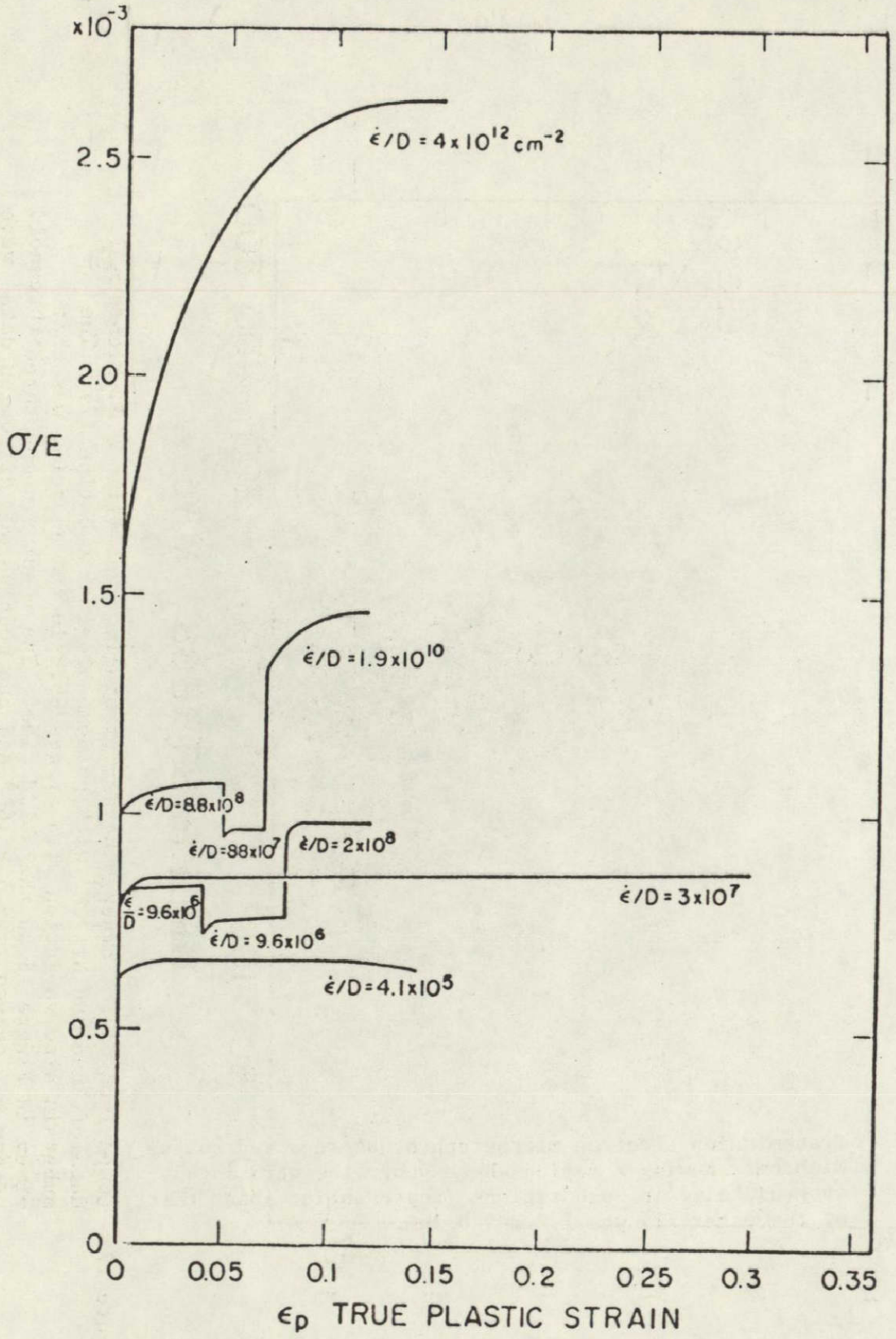

Figure 16. Compression true stress-true strain curves for coarse grain T. D. Nichrome plotted as modulus compensated stress versus strain. Negligible strain hardening is observed if the value of $\dot{\epsilon}/D$ is below the intersection stress (Figure 14), i.e., below $\dot{\epsilon}/D = 2 \times 10^{9} cm^{-2}$. At $\dot{\epsilon}/D$ values above the intersection stress, strain hardening dominates the stress-strain curves. This observation is in agreement with our prediction that a constant structure exists at low stress but will be refined at high stresses where the equilibrium subgrain size is finer than the original subgrain size, data from Hausselt and Nix[73] and change in strain rate tests from this investigation.

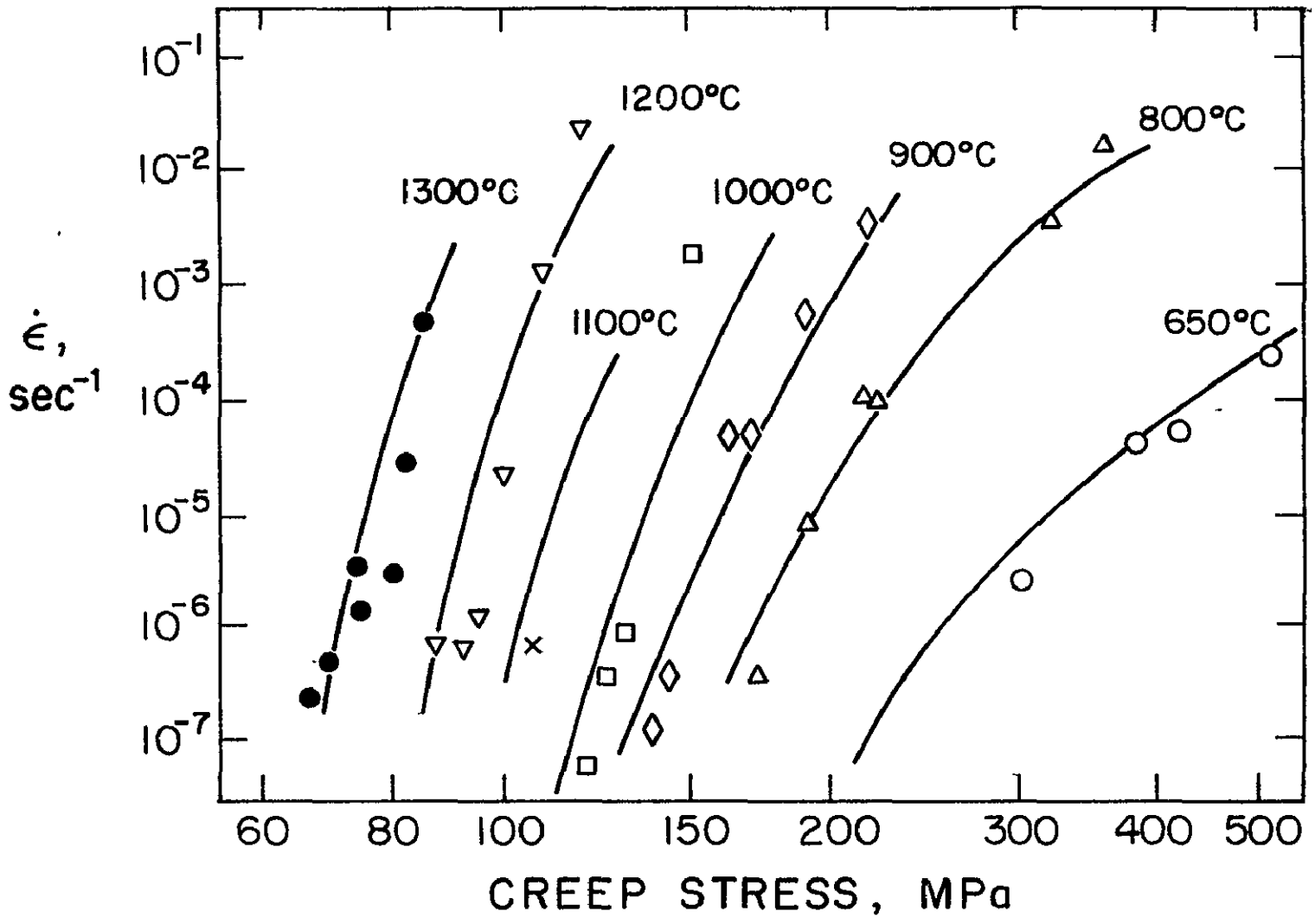

Figure 17. Comparison of the creep behavior of single crystalline T.D. Nichrome data of Lund and Nix[16] with phenomenological equation (7). The subgrain size variation with stress used in the equation was that given in Figure 13 as the solid line. The modulus compensated threshold stress was chosen as 5.5×10^{-4} and the modulus and diffusion data were taken from references 28, 29 and 30. The predicted behavior as given by the lines agrees remarkably well with the experimental data.

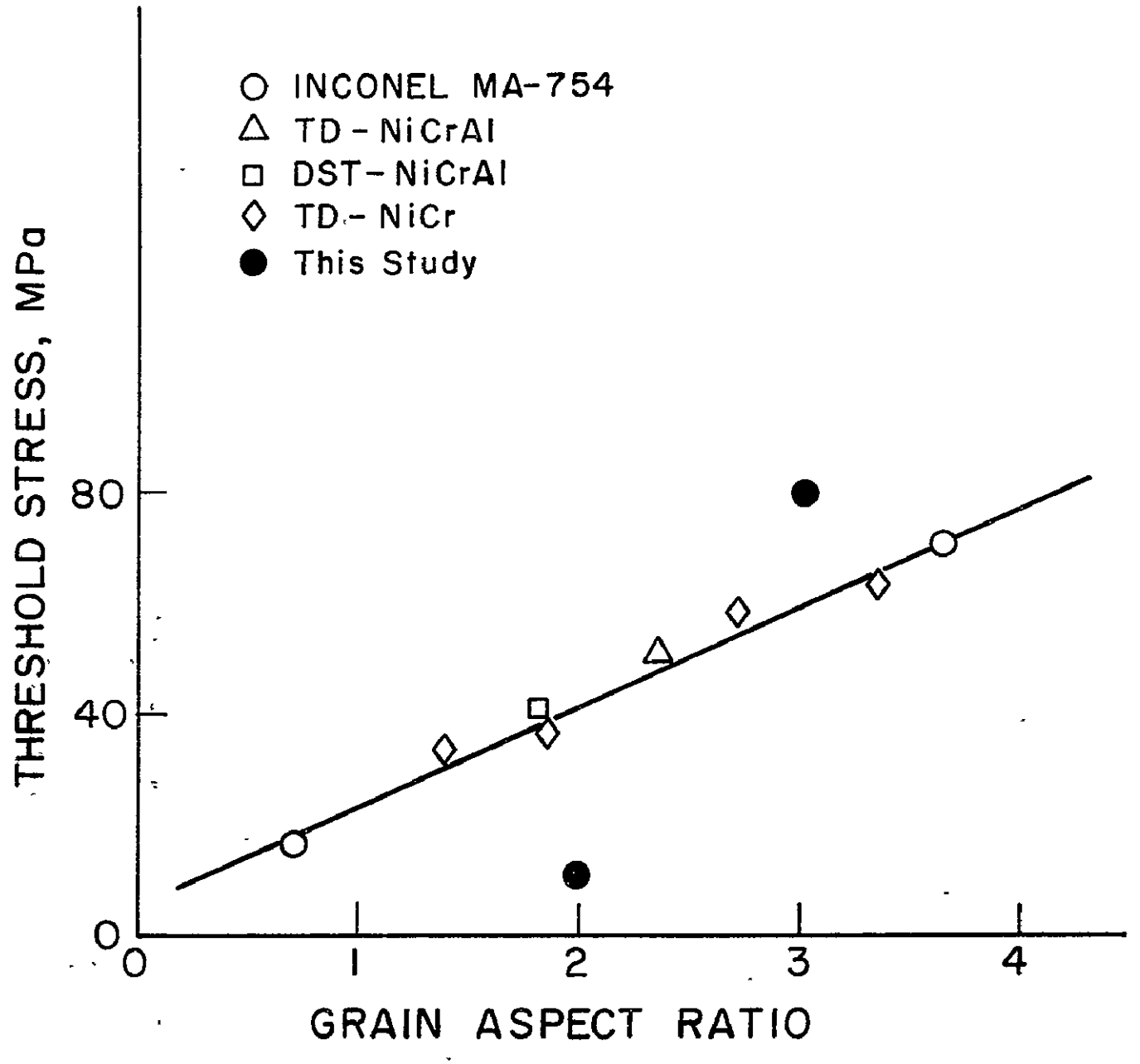

Figure 18. Threshold stress for various nickel base alloys at 1093°C as a function of grain aspect ratio as given by Whittenberger[27]. The threshold stresses for our fine and coarse grain size T. D. Nichrome materials are plotted as solid symbols for comparison.

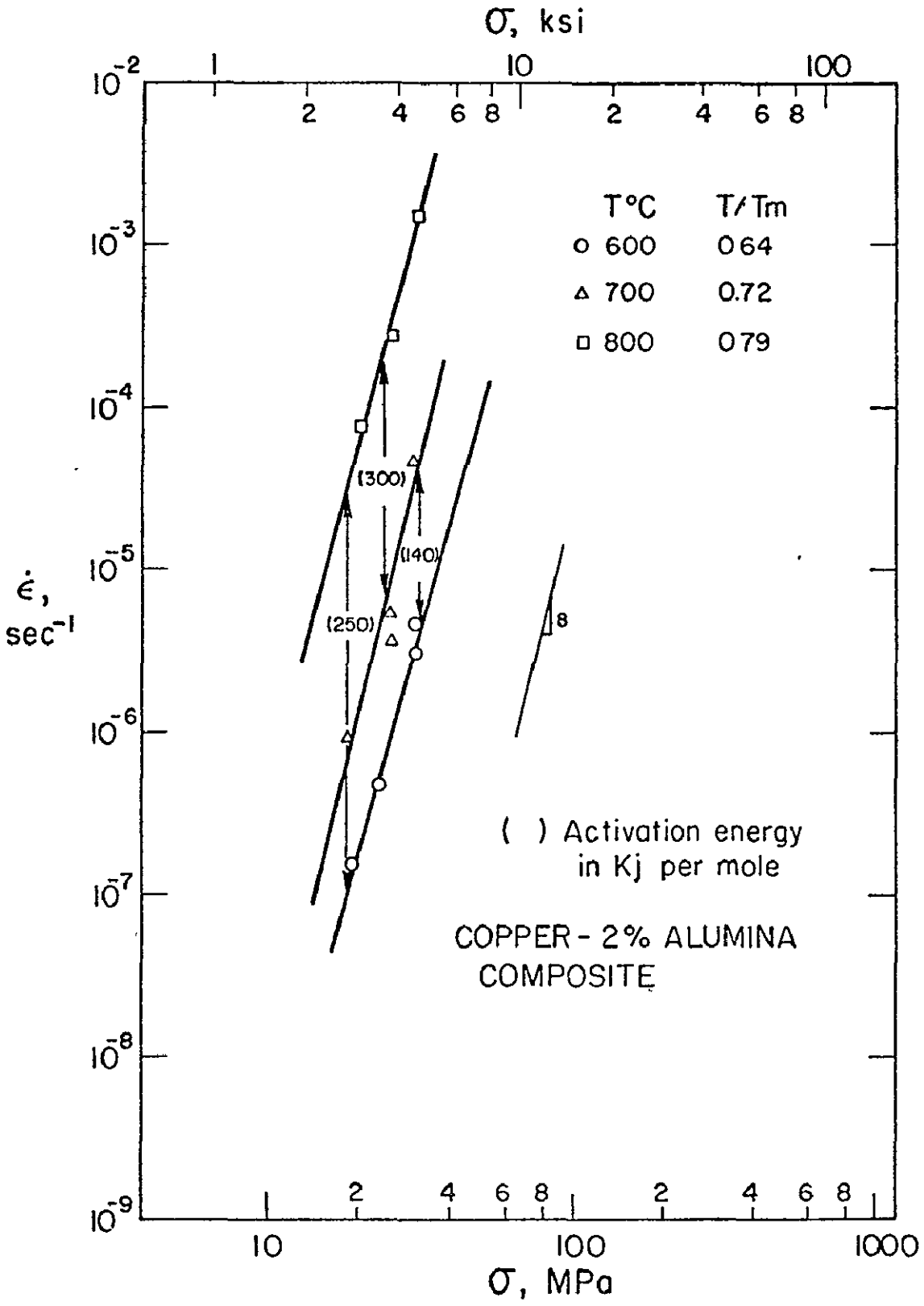

Figure A1. Flow stress-strain rate relation for copper-2% alumina composite. The average activation energy for creep is about 250 kjoules per mole which is above that for lattice self diffusion in copper (195 kjoules per mole)[47].

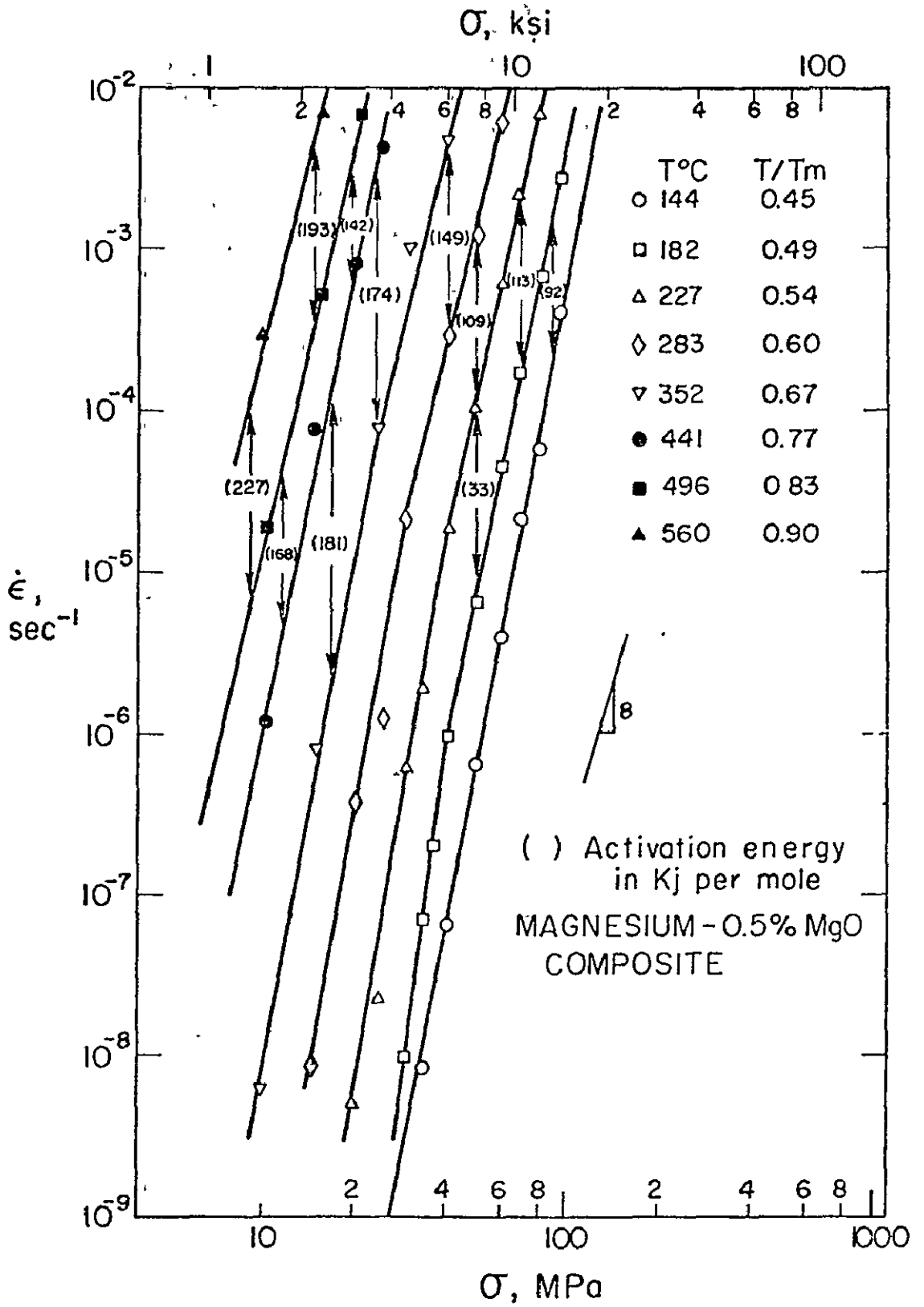

Figure A2. Flow stress-strain rate relation for magnesium -0.5% MgO composite.[44] The average activation energy for creep above 0.6 T_m is 175 kjoules per mole which is above that for lattice self diffusion (135 kjoules per mole)[49]. The activation energy below 0.5 T_m is 92 kjoules per mole which is about equal to that for dislocation pipe diffusion (95 kjoules per mole).

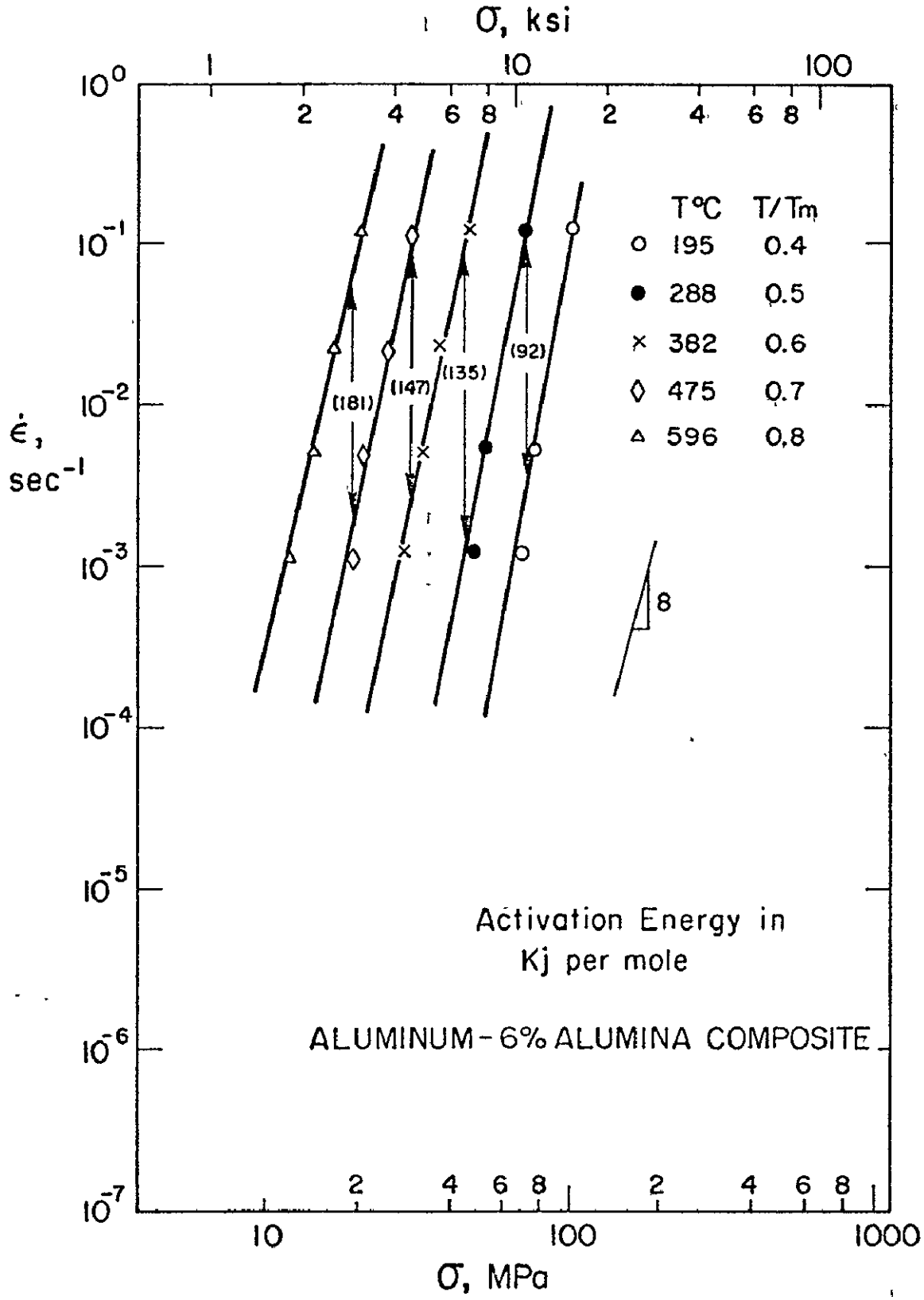

Figure A3. Flow stress-strain rate relation for aluminum-6% alumina composite.[45] The average activation energy for creep above 0.6 T_m is 165 kjoules per mole which is above that for lattice self diffusion in aluminum (140 kjoules per mole)[4,50].

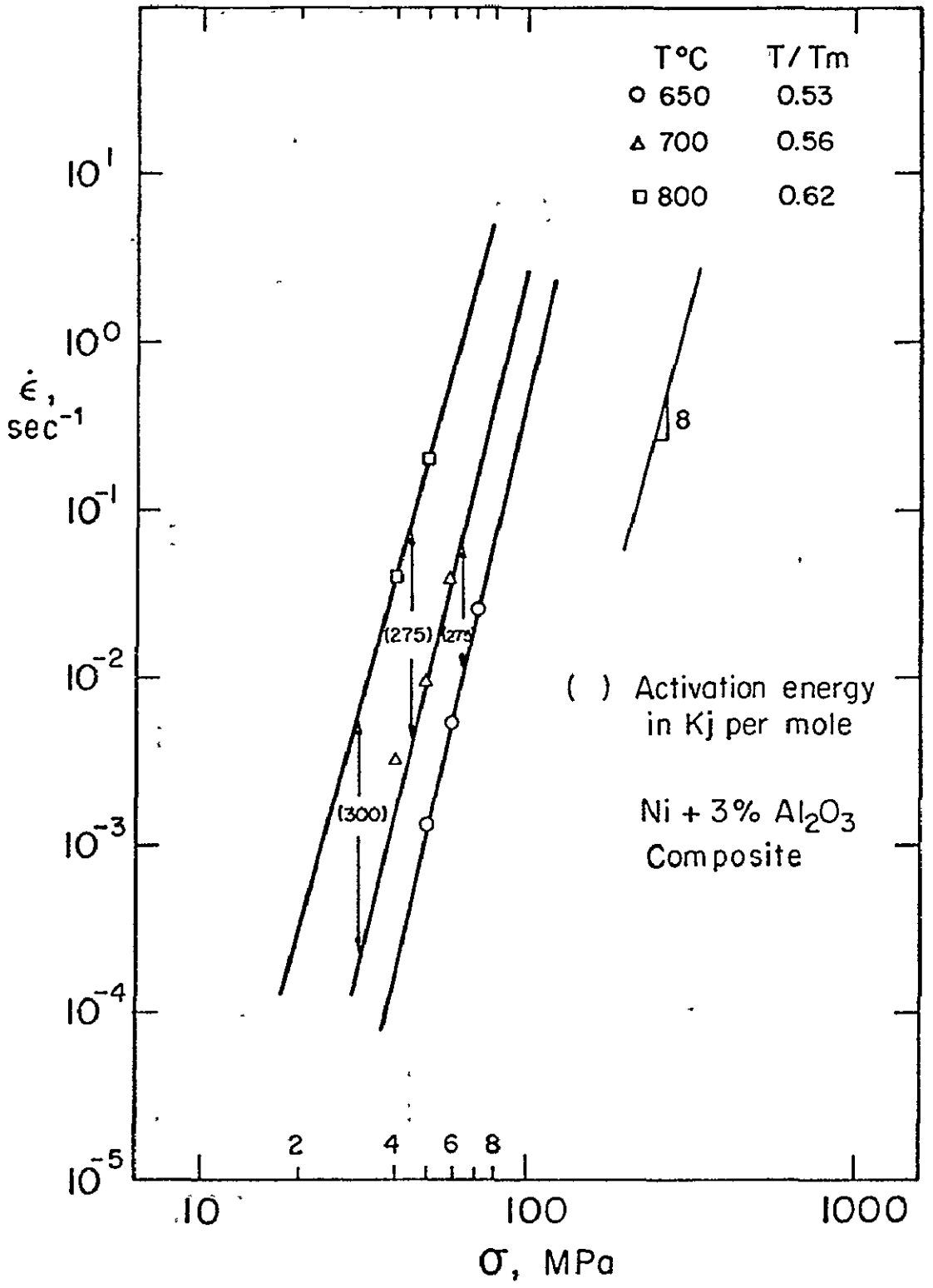

Figure A4. Flow stress-strain relation for nickel-3% alumina composite.[46] The average activation energy for creep is 285 kjoules per mole, which is equal to that for lattice self diffusion in nickel[54].

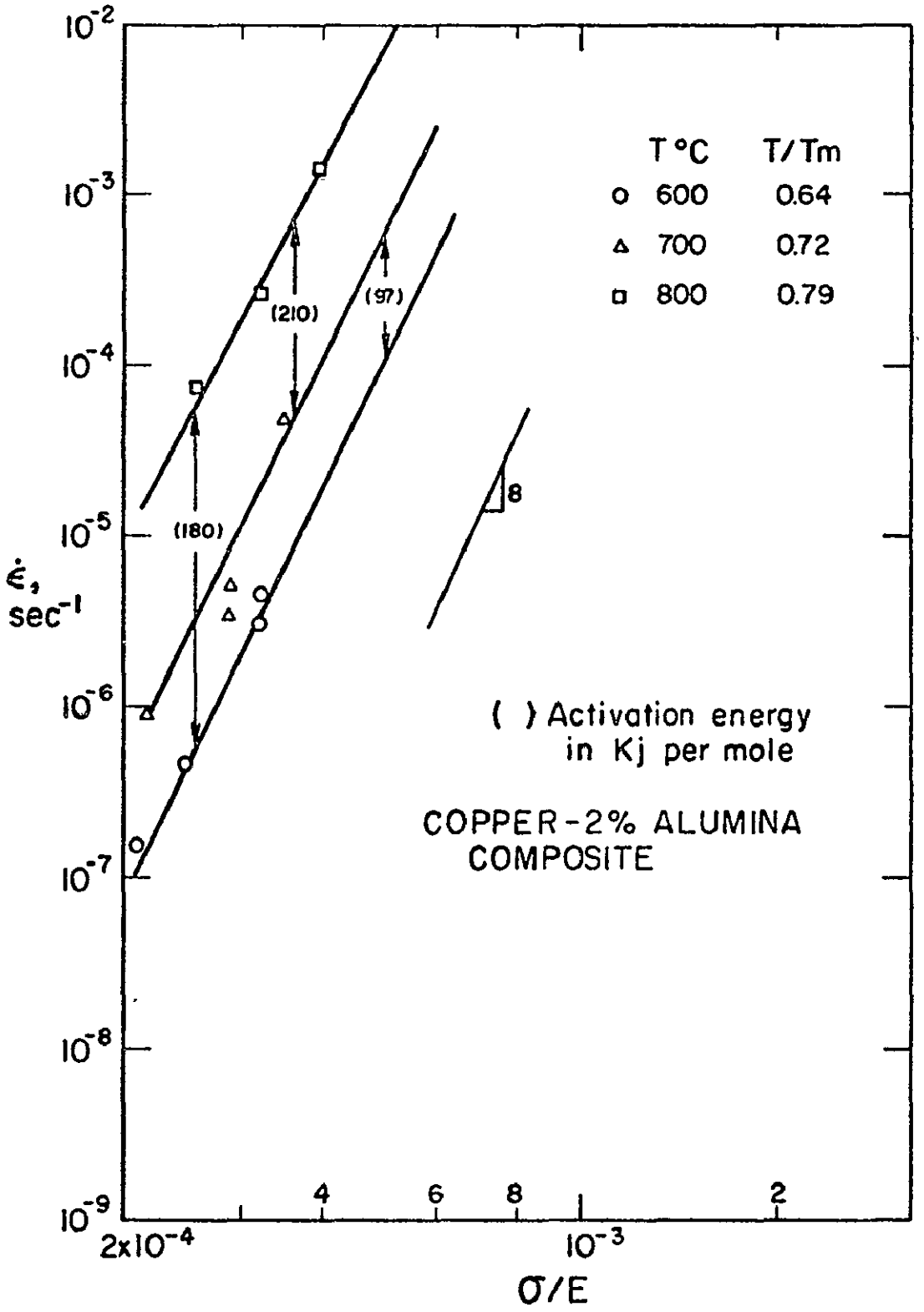

Figure A5. Modulus compensated flow stress-strain rate relation for copper-2% alumina composite.[42] The average activation energy is 180 kjoules per mole, which is about equal to that for lattice self diffusion in copper (195 kjoules per mole)[47].

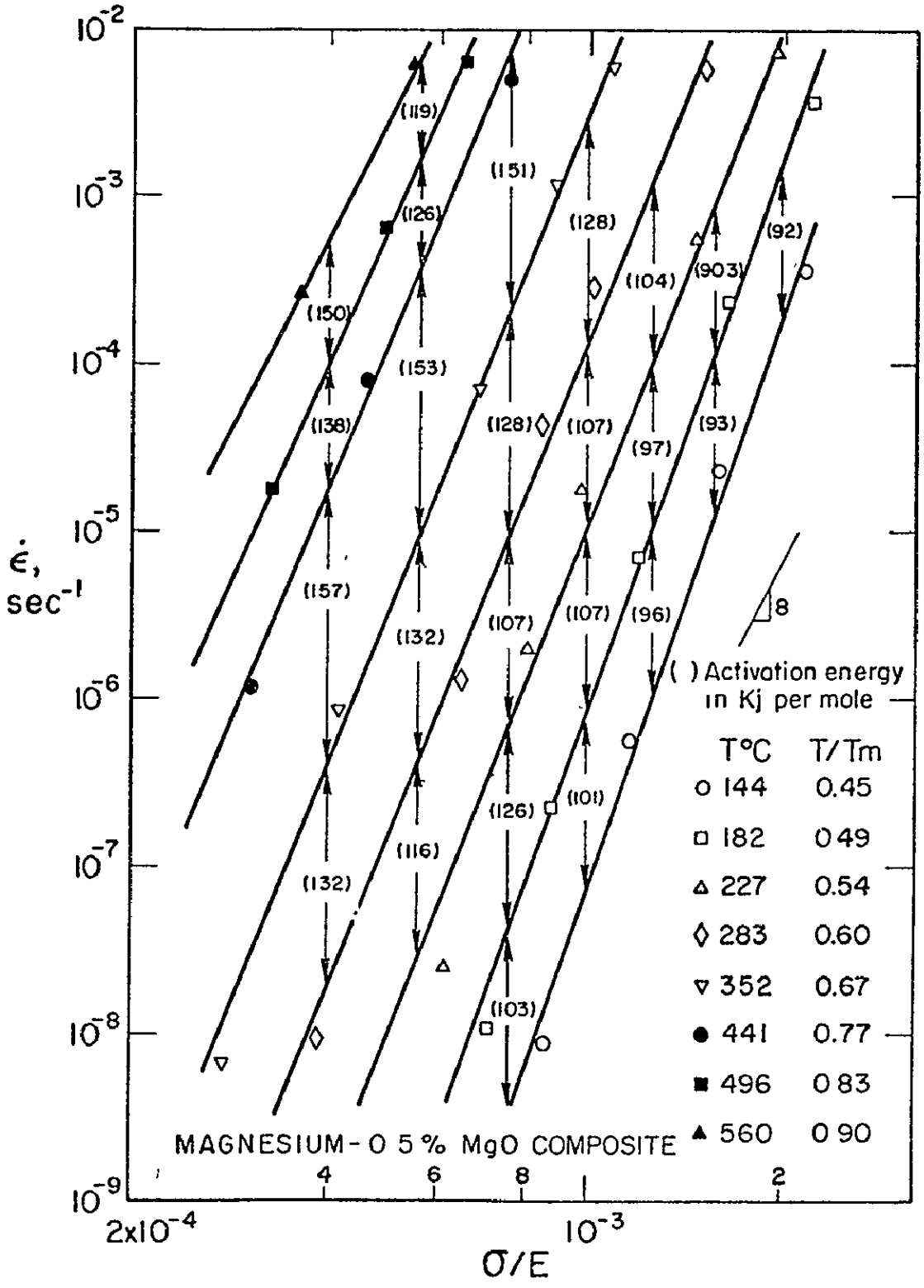

Figure A6. Modulus compensated flow stress-strain rate relation for magnesium-0.5% MgO composite.[44] The average activation energy for creep is about 135 kjoules per mole above 0.6 T_m, which is equal to that for lattice self diffusion in magnesium.[49] The average activation energy for creep is 95 kjoules per mole below 0.5 T_m, which is about equal to that for dislocation pipe-diffusion.

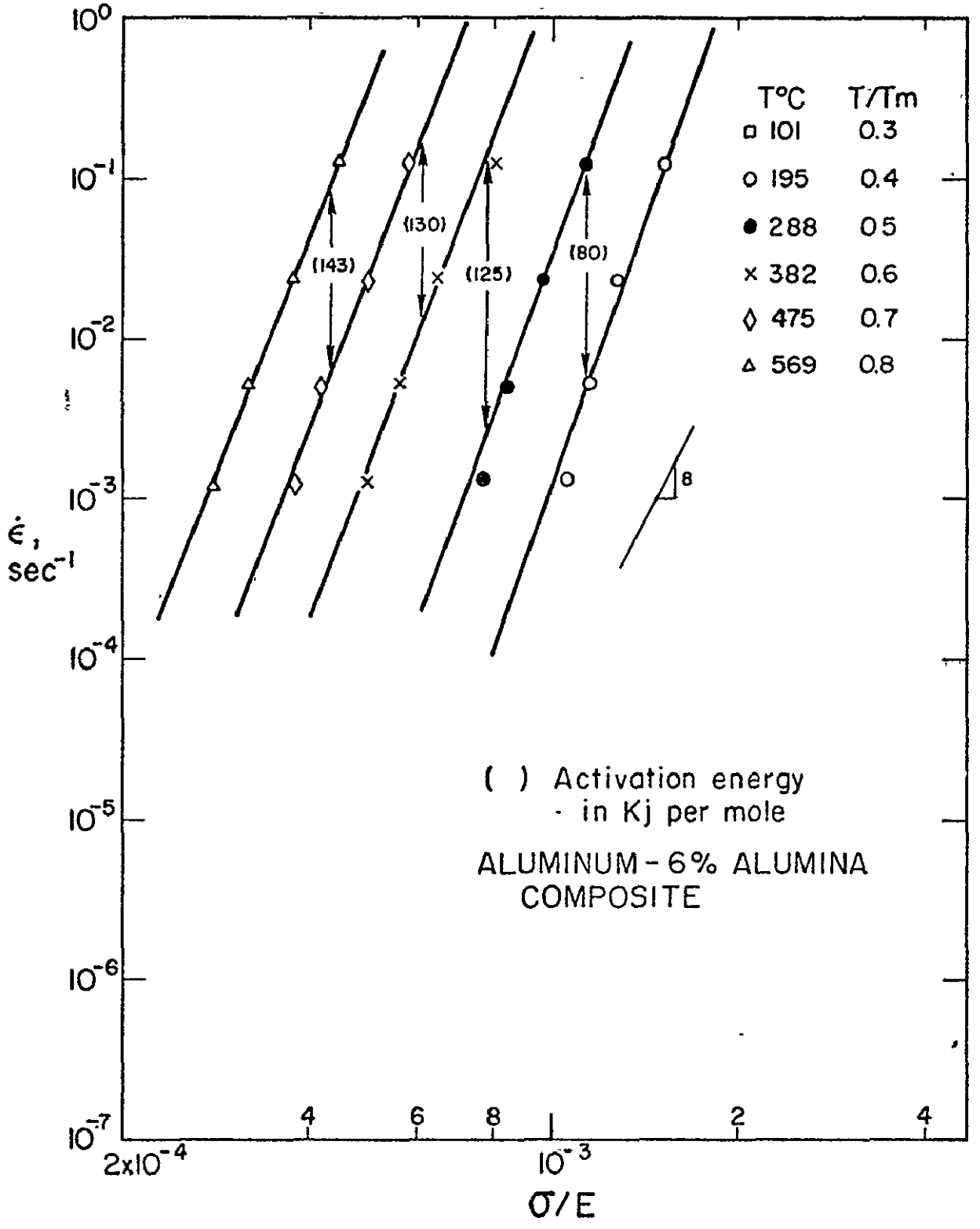

igure A7. Modulus compensated flow stress-strain rate relation for aluminum-6% alumina composite.[45] The average activation energy for creep above 0.6 T_m is 135 kjoules per mole, which is about equal to that for lattice self-diffusion in aluminum (140 kjoules per mole)[50].

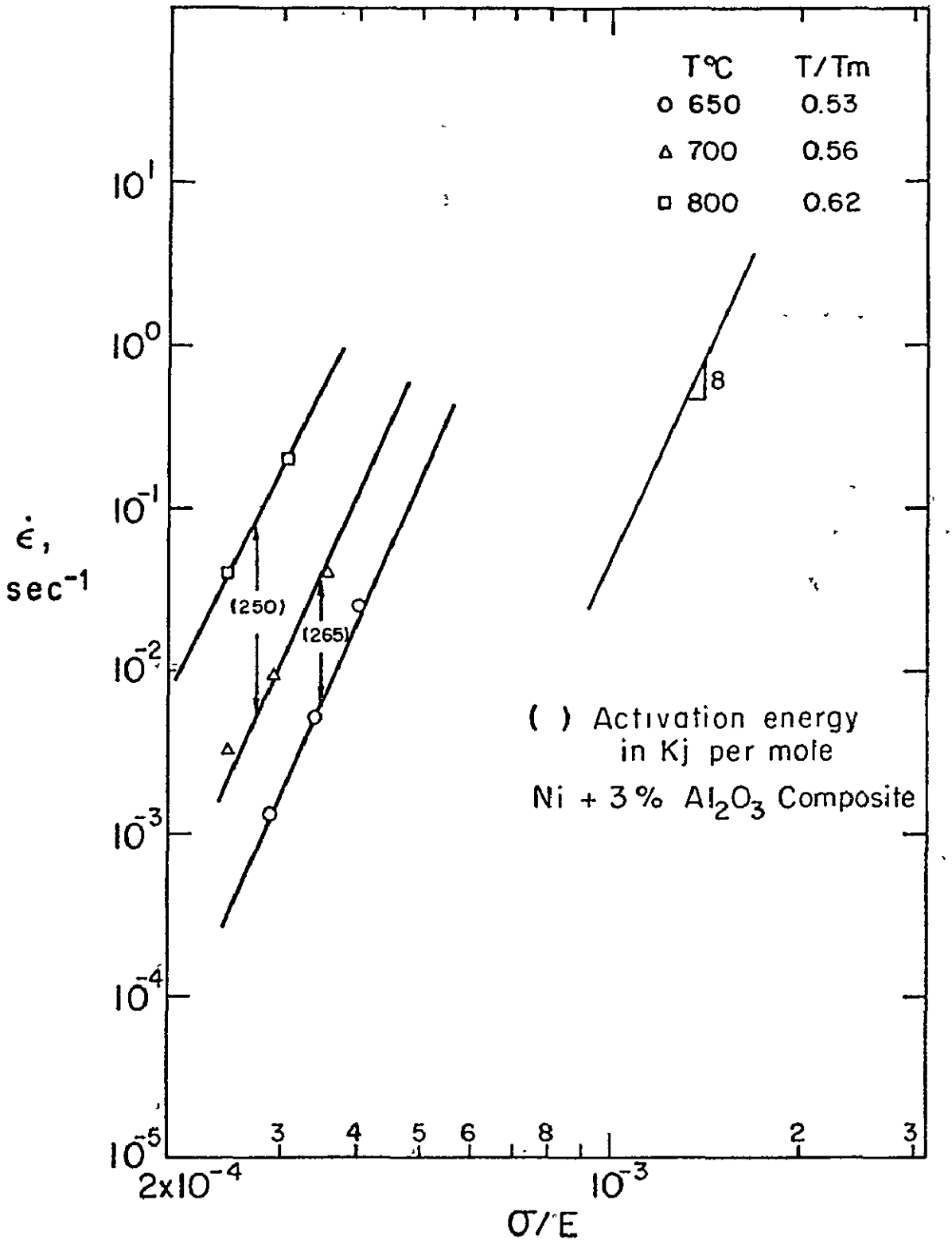

Figure A8. Modulus compensated flow stress-strain rate relation for nickel-3% alumina composite.[46] The average activation energy for creep is about 255 kjoules per mole, which is slightly below that for self-diffusion in nickel (285 kjoules per mole)[51]. This can be related to the contribution of pipe diffusion at temperature below 0.6 T_m.

1 Report No	2 Government Accession No	3 Recipient's Catalog No
NASA CR-135432		

4 Title and Subtitle	5 Report Date
CREEP OF OXIDE DISPERSION STRENGTHENED MATERIALS (WITH SPECIAL REFERENCE TO T. D. NICHROME)	June 1978
	6 Performing Organization Code
7 Author(s)	8 Performing Organization Report No
Jerhong Lin and Oleg D. Sherby	
	10 Work Unit No
9 Performing Organization Name and Address	
Department of Material Science and Engineering Stanford University Stanford, California 94305	11 Contract or Grant No NGR-05-020-671
	13 Type of Report and Period Covered
12 Sponsoring Agency Name and Address	Contractor Report
National Aeronautics and Space Administration Washington, D.C. 20546	14 Sponsoring Agency Code

15 Supplementary Notes

Final report. Project Manager, J. Daniel Whittenberger, Materials and Structures Division, NASA Lewis Research Center, Cleveland, Ohio 44135.

16 Abstract

It is shown that the creep behavior of oxide dispersion strengthened (ODS) alloys is controlled principally by the creep properties of the matrix of the alloy devoid of particles. Thus, diffusion-controlled slip processes determine the rate controlling step in such materials. The role of the particles is to stabilize a fine substructure which is invariant with the creep stress over a wide range of stress. This characteristic leads to negligible strain hardening during creep and suggests that creep relations developed for pure metals and many solid solution alloys at constant structure should be used to describe the creep of ODS alloys. A second characteristic of the ODS alloys is that a stress may exist below which creep will not occur (threshold stress). These characteristics lead to the following phenomenological relation to describe the creep rate of the ODS materials:

$$\dot{\epsilon} = K\left(\frac{\lambda}{b}\right)^3 \frac{D_{eff}}{b^2}\left(\frac{\sigma - \sigma_o}{E}\right)^8$$

where λ is the subgrain or barrier distance, D_{eff} is the effective diffusion coefficient, E is the dynamic unrelaxed Young's modulus, b is the burgers vector, σ_o is the threshold stress, and K is a material constant equal to 10^9 for high stacking fault energy materials. At high stresses, the well-defined subgrain initially present in ODS alloys may be coarser than the equilibrium subgrain size that may develop in the matrix of the material. In this high stress range, the creep rate of ODS alloys will follow the behavior of the matrix material devoid of oxide particles. These predictions have been shown to predict the creep behavior of polycrystalline and single crystalline T. D. Nichrome.

17 Key Words (Suggested by Author(s))	18 Distribution Statement
Mechanical properties; Oxide dispersion strengthened alloys; High temperature; Nichrome; TD-NiCr; ODS alloys	Unclassified - unlimited STAR Category 26

19 Security Classif (of this report)	20 Security Classif (of this page)	21 No of Pages	22 Price*
Unclassified	Unclassified	61	

* For sale by the National Technical Information Service, Springfield, Virginia 22161

NATIONAL AERONAUTICS AND SPACE ADMINISTRATION
WASHINGTON, D C 20546

OFFICIAL BUSINESS
PENALTY FOR PRIVATE USE $300

SPECIAL FOURTH-CLASS RATE
BOOK

POSTAGE AND FEES PAID
NATIONAL AERONAUTICS AND
SPACE ADMINISTRATION
451

U.S. MAIL

POSTMASTER

If Undeliverable (Section 158
Postal Manual) Do Not Return